Non-specific interference of cobalt with siderophore-dependent iron uptake pathways

Ana Carballido Lopez, Olivier Cunrath, Anne Forster, Julien Pérard, Gwenaëlle Graulier, Rachel Legendre, Hugo Varet, Odile Sismeiro, Quentin Perraud, Bénédicte Pesset, et al.

Non-specific interference of cobalt with siderophore-dependent iron uptake pathways

CARBALLIDO LOPEZ, Ana, CUNRATH, Olivier, FORSTER, Anne, PÉRARD, Julien, GRAULIER, Gwenaëlle, LEGENDRE, Rachel, VARET, Hugo, SISMEIRO, Odile, PERRAUD, Quentin, PESSET, Bénédicte, SAINT AUGUSTE, Pamela, BUMANN, Dirk, MISLIN, Gaetan, COPPEE, Jean Yves, MICHAUD-SORET, Isabelle, FECHTER, Pierre et SCHALK, Isabelle

[a]Université de Strasbourg, UMR7242, ESBS, Bld Sébastien Brant, F-67413 Illkirch, Strasbourg, France.

[b]CNRS, UMR7242, ESBS, Bld Sébastien Brant, F-67413 Illkirch, Strasbourg, France.

[c]Univ-Grenoble alpes, CNRS, CEA, BIG, CBM, CEA-Grenoble, 38000 Grenoble, France.

[d]Transcriptome and EpiGenome, Biomics, Institut Pasteur, 28 rue du Docteur Roux, 75015 Paris, France.

[e]Institut Pasteur – Bioinformatics and Biostatistics Hub – C3BI, USR 3756 IP CNRS – Paris, France.

[f]Focal Area Infection Biology, Biozentrum, University of Basel, Basel, Switzerland

To whom correspondence should be addressed: Isabelle J. Schalk, UMR 7242, IREBS, ESBS, Blvd Sébastien Brant, CS 10413, F-67412 Illkirch, Strasbourg, France. Tel: 33 3 68 85 47 19; Fax: 33 3 68 85 48 29; E-mail: isabelle.schalk@unistra.fr or p.fechter@unistra.fr

Abstract

Much data shows that biological metals other than Fe^{3+} can interfere with Fe^{3+} acquisition by siderophores in bacteria. Siderophores are small Fe^{3+} chelators produced by the microorganism to obtain access to Fe^{3+}. Here, we show that Co^{2+} is imported into *Pseudomonas aeruginosa* cells in a complex with the siderophore pyochelin (PCH) by the ferri-PCH outer membrane transporter FptA. Moreover, the presence of Co^{2+} in the bacterial environment strongly affects the production of PCH. Proteomic and transcriptomic approaches showed that a decrease of PCH production is associated with repression of the expression of the genes involved in PCH biosynthesis. We used various molecular biology approaches to show that this repression is not Fur- (Ferric uptake transcriptional regulator) dependent but due to competition of PCH-Co with PCH-Fe for PchR (transcriptional activator), thus inhibiting the formation of PchR-PCH-Fe and consequently the expression of the PCH genes. We observed a similar mechanism of repression of PCH production, but to a lesser extent, by Ni^{2+}, but not for Zn^{2+}, Cu^{2+}, or Mn^{2+}. Here, we show, for the first time at a molecular level, how the presence of a contaminant metal can interfere with Fe^{3+} acquisition by the siderophores PCH and PVD.

Introduction

In living organisms, interactions between biomolecules and biological metals (Na, Mg, K, Ca, Mn, Fe, Zn, Ni, Cu, Co, and Mo) are vital and play a role in macromolecule structure and cell metabolism. For example, one third of proteins require metals for their effective functioning. The interactions between macromolecules and metals are highly specific. Waldron and Robinson proposed that to ensure that each metalloprotein or metalloenzyme in bacteria binds the correct metal and functions properly, 'metals are not in competition for a limited pool of proteins, but rather the proteins compete for a limited pool of metals in the cells'.[2,3] Therefore, any disequilibrium of this limited intracellular pool of metals (the bacterial metallome) affects bacterial cell viability. However, bacteria are often subject to variations in metal concentrations in their environment, including during infections, in which they may be confronted with "nutriment immunity", whereby the host uses deprivation of, or poisoning with, metals as defense strategies against microbial invaders.[4,5] For example phagocytes use Cu and/or Zn intoxication to reduce the intracellular survival of pathogens.[6] How bacteria cope with such metal concentration disequilibria at the molecular level and the cross-talk to maintain homeostasis of different biological metals in bacterial cells are still poorly understood.

Bacterial iron homeostasis has attracted the most attention over the last decades. Iron is a key nutriment for bacterial growth, which is paradoxically poorly bioavailable because of its very low solubility under aerobic conditions and physiological pH. Thus, to gain access to Fe^{3+}, most bacteria produce siderophores.[7] These compounds have various chemical structures, a molecular weight usually between 200 and 2 000 Da, and are characterized by an extremely high affinity for Fe^{3+}, with, for example, K_a values of 10^{43} for the siderophores enterobactin.[8] Siderophores provide bacteria with Fe^{3+} by scavenging this metal from the bacterial environment and transporting it into either the bacterial periplasm or cytoplasm.[9,10] This strategy works in any bacterial environment, such as in the rhyzosphere[11], but also plays a key role in the host during infections.[12] *P. aeruginosa*, an opportunistic pathogen and used as a model in the present study, produces two major siderophores, pyoverdine

(PVD) and pyochelin (PCH) (Figure 1).[9] The synthesis of these chelators is correlated with the concentration of iron, both in bacterial cells and the environment.[13] In media with moderately low concentrations of iron (approximately 300 nM), *P. aeruginosa* cells produce more PCH than PVD, whereas in more severely iron-restricted media (approximately 20 nM), PCH production remains highly active and, in addition, PVD production is strongly stimulated.[13,14]

Fe^{3+} uptake into bacteria *via* siderophores always involves a siderophore-specific TonB-dependent transporter for its uptake across the outer membrane in Gram-negative bacteria.[15] Depending on the siderophore, Fe^{3+} is then either delivered into the bacterial periplasm or cytoplasm. Transport into the cytoplasm involves further transport of the ferri-siderophore complex across the inner membrane *via* proton motive force-dependent permeases or ABC transporters.[16] Iron release from siderophores in the bacterial periplasm or cytoplasm requires Fe^{3+} reduction (siderophores having a lower affinity for Fe^{3+} compared to Fe^{2+}), often associated with chemical modification or hydrolysis of the siderophores.[16] Siderophore production is generally negatively regulated by the presence of Fe^{2+} *via* the Fur transcriptional regulator[19] and positively by iron restriction and the response of various regulatory systems, such as sigma and anti-sigma factors[20], the AraC regulators, or two component systems.[21] Under iron starvation, PCH production is activated via the action of the AraC regulator PchR and PVD by anti-sigma (FpvR) and sigma factors (PvdS and FpvI).[21–23]

An increasing number of studies have also reported that siderophores are able to chelate efficiency metals other than Fe^{3+}.[18] Previously, using the spectral properties of PVD and PCH, we have shown that both PVD and PCH are able to chelate the biological metals Co^{2+}, Cu^{2+}, Ni^{2+} and Zn^{2+} as well as metals like Ag^{+}, Pb^{2+}, Al^{3+}.[24,25] PVD chelates metals with a 1 : 1 stoechiometry and stability constants have been determined for some PVD-metal complexes: PVD-Fe (Ka = $10^{30.8}$ M^{-1}), PVD–Ni^{2+} (Ka = $10^{10.9}$ M^{-1}), PVD–Cd^{2+} (Ka = $10^{8.2}$ M^{-1}), PVD-Cu^{2+} (Ka = $10^{20.1}$ M^{-1}).[26,27] PCH forms predominantly 1 : 2 (M^{2+} /PCH) complexes and the stability constant determined are: for Fe^{3+} (Ka = $10^{28.8}$ M^{-2}), for Zn^{2+} (Ka = $10^{26.0}$ M^{-2}) and for Cu^{2+} (Ka = $10^{25.0}$ M^{-2}).[28] Baysse *et al.* have shown that PCH can also bind the transition metal

vanadium generating a Fenton reaction in the cells.[29] Moreover several studies have shown that the presence of metals other than Fe^{3+} in the bacterial environment can modulate the bacterial production of siderophores, but nothing is known concerning the molecular mechanisms involved.[30–32] For example, PCH synthesis in *P. aeruginosa*, is repressed by 10 μM Fe^{2+}, Co^{2+}, Mo^{+6}, Ni^{2+}, and Cu^{2+}.[33,34] At last, an increasing number of studies have reported that siderophores, in addition to their important role in Fe^{3+} acquisition, also protect bacterial cells against excess toxic metals present in their environment and can consequently play a role in bacterial metal resistance.[13,17,18] Previous studies by our group have shown that both PVD and PCH protect *P. aeruginosa* from toxic metals or an excess of essential metals, to a similar extent, by preventing their intracellular accumulation, thus maintaining the homeostasis of the various biological metals present in bacterial cells.[13,17]

To better understand the possible role of PVD and PCH in the homeostasis of biological metals other than iron, we explored the effect of the presence of various biological metals (Co^{2+}, Cu^{2+}, Ni^{2+}, Mn^{2+} and Zn^{2+}) in bacterial growth media on PVD and PCH production and investigated the possible molecular mechanisms involved in the phenotype(s) observed. Heavy metals were not included in our study, the possible role of the two siderophores in heavy metal resistance being not the focus of this work. We observed that Co^{2+} repressed PCH synthesis with the same efficiency as Fe^{3+}, and repression was also observed with Ni^{2+}, but with lower efficiency. There was no repression by Zn^{2+}, Mn^{2+}, or Cu^{2+}. The repression observed is Fur-independent and due to the ability of Co^{2+} and Ni^{2+} to interfere with the transcriptional regulator PchR (activator of PCH production, Scheme 1). Co^{2+} and Ni^{2+} inhibit PchR-PCH-Fe formation and consequently the concentration of this complex in bacterial cells decreases, resulting in a decrease of the transcription of the genes encoding the enzymes involved in PCH synthesis.

Materials and methods

Chemicals. The metals used were in the following forms: $CoCl_2$,$6H_2O$ (Strem Chemicals), $CuCl_2$,$2H_2O$ (Strem Chemicals), $NiCl_2$,$6H_2O$ (Strem Chemicals), $FeCl_3$ (Alfa Aesar), $Mn(OAc)_2$,$4H_2O$ (Strem Chemicals) and $ZnCl_2$ (Strem Chemicals). All solutions were prepared at concentrations between 1 nM and 100 µM in 0.5 N HCl or 0.5 N HNO_3. These stock solutions were then diluted with 50 mM Tris-HCl pH 8.0. The PCH used in these experiments was synthesized according to a previously published protocol.[35]

Bacterial strains and growth media. *P. aeruginosa* strains used throughout this study are shown in Table 1. For cultures of *P. aeruginosa* strains in iron-limited media, bacteria were first grown in LB broth overnight at 30°C. The bacteria were then washed in CAA medium (casamino acid medium, composition: 5 $g.L^{-1}$ low-iron CAA (Difco), 1.46 $g.L^{-1}$ K_2HPO_4 $3H_2O$, 0.25 $g.L^{-1}$ $MgSO_4$ $7H_2O$), diluted two-fold and incubated for 24 h at 30°C.

Siderophore quantification. The production of PCH and PVD were evaluated as described previously.[25-36] PVD production was monitored by its characteristic absorbance of 400 nm at neutral pH.[36] PCH has a characteristic absorbance of 320 nm, but unlike PVD, this siderophore cannot be detected directly in the bacterial growth medium and needs first to be extracted from the cultures and concentrated before absorbance monitoring.[13,36]

UV and fluorescence spectra of PCH-metal complexes. PCH was solubilized in methanol and PCH-metal complexes were prepared in methanol by mixing 1 eq. of metal with 2 eq. of PCH. 50 mM TrisHCl pH 8.0 buffer was added to reach a concentration of PCH-metal complexes of 50 µM. UV spectra were measured on a Nanodrop 2000 spectrophotometer and fluorescence spectra were measured on a TECAN M200 multiplate reader. All measures were carried out in 50 mM TrisHCl buffer. For emission spectra : λ_{exc} = 350 nm; for excitation spectra : λ_{em} = 422 nm.

Bacterial growth and quantification of fluorescence intensity. Cells were cultured overnight in CAA medium, pelleted by centrifugation, resuspended in fresh CAA medium, and the resulting suspension diluted so as to obtain an optical density at 600 nm of 0.01 units. We dispensed 200 µL of the suspension per well into a 96-well plate (Greiner, U-bottomed microplate) with or without the different metals tested. The plates were incubated at 30°C, with shaking, in a Tecan microplate reader (Infinite M200, Tecan) for measurements of OD_{600nm} and mCherry (excitation/emission wavelengths: 570 nm/610 nm) fluorescence at 30-min intervals, for 40 h. We calculated the mean of three replicates for each measurement.

***Proteomics analysis*.** Bacteria were grown in CAA medium as described above (for growth curve see Figure 1SM in Supplementary Materials). After the first overnight culture in CAA medium, the bacteria were diluted in 10 mL CAA to an $OD_{600\ nm}$ of 0.1 and incubated with or without 10 µM Fe^{3+} or Co^{2+} for 8 h at 30°C. For the digestion and cleanup steps, the same strategy was used as previously described.[37] For the shotgun proteomics assays, 1 µg of peptides of each sample were subjected to LC–MS (liquid chromatography-mass spectrometry) analysis using the same approach as previously described.[37]

Transcriptomic analysis. Bacteria were grown in CAA medium exactly as described above for the proteomic analyses and harvested after 8 h of cultures at 30°C. The total RNA were extracted by hot phenol treatment. Briefly, an aliquot of 8 x 10^8 cells from the cultures were added to two volumes of RNAprotect Bacteria Reagent (Qiagen). After centrifugation, the cell pellets were dissolved in 1 ml of lysis buffer (300 mM NaCl ; 1% SDS ; 8 mM EDTA), incubated at 90°C for 1 min before the addition of 1 mL of phenol and a further incubation at 65°C for 10 min. The extracted RNAs (aqueous phase) were purified again with 1 volume of Phenol/Chloroform. To eliminate any DNA traces, the RNAs were submitted twice to DNaseI treatment. The RNAs were then submitted to ribosomal depletion using the RiboZero Bacteria kit (Illumina). The efficiency of depletion was validated on a Bioanalyzer nanochip (Agilent). Directional cDNA libraries for sequencing were constructed using the TruSeq

Stranded RNA LT Sample Prep kit (Illumina) from enriched non-rRNA samples, following the manufacturer's instructions. After validation of the libraries on a Bioanalyzer DNA1000 chip (Agilent) and QuBit (Invitrogen) quantification, sequencing was performed on a HiSeq 2500 (Illumina). Reads were 65 bp-long in single mode.

Count data were analyzed using R version 3.3.1[38] and the Bioconductor package DESeq2 version 1.12.4.[39] Normalization and the estimation of dispersion were performed with DESeq2, using the default parameters, and statistical tests for differential expression were performed, applying the independent filtering algorithm. A generalized linear model was used to test for the differential expression between the three biological conditions: PAO1 without metals, PAO1 in the presence of Co^{2+} or Fe^{3+}. For each pairwise comparison, raw p-values were adjusted for multiple testing according to the Benjamini and Hochberg (BH) procedure[40] and genes with an adjusted p-value lower than 0.05 were considered to be differentially expressed.

Reads were cleaned of adapter sequences and low-quality sequences using an in-house program (https://github.com/baj12/clean_ngs). Only sequences at least 25 nt in length were considered for further analysis. Bowtie version 0.12.7[41], with default parameters, was used for alignment on the reference genome (*Pseudomonas aeruginosa* PAO1 from NCBI). Genes were counted using featureCounts version 1.4.6-p3[42] from Subreads package (parameters: -t gene -s 1).

Metal quantification by ICP-AES. PCH-metal complexes were prepared by incubating PCH solubilized in methanol with $FeCl_3$, $CoCl_2$, $NiCl_2$ or $ZnCl_2$ at a molar ratio of 2:1 for 15 min. Tris-HCl (50 mM) pH 8.0 buffer was added to bring the siderophore-metal complexes to a final concentration of 4 mM. Δ*pvdF*Δ*pchA* and Δ*pvdF*Δ*pchA*Δ*fptX* cells were grown overnight in CAA media as described above. Cells were then washed and resuspended in CAA medium at an $OD_{600\ nm}$ of 1.5. PCH-Fe or PCH-Co were added to a final concentration of 4 µM and the solutions incubated for 30 min at 30°C with shaking. The samples were then centrifuged and the bacterial pellets washed once with ultrapure water and dried at 50°C for 48 h. Cells were mineralized by incubation in 70% (v/v) HNO_3 for 48 h at room

temperature. The volume was brought up to 10 mL with ultrapure water and the samples filtered through a membrane with a 0.22 µm syringe filter unit. The samples were then analyzed with an ICP-AES apparatus (Varian 720 ES) at the following wavelengths (nm): Co (228.62), Fe (238.20), Ca (393.37), Cd (214.44), Co (228.62), Cr (267.72), Cu (327.40), Fe 238.20), K 766.49), Mg (279.55), Mn (257,61), Mo (202.03), Na (589.59), Ni (231.60), Pb 220.35), V (292.40), and Zn (213.86).

For the data in Figure 4, bacteria were grown in CAA medium in the presence of 5 µM $CoCl_2$. At the end of the exponential phase, samples were centrifuged, and the bacterial pellets treated as described above for the experiment with PCH-Co or PCH-Ni complexes.

$^{55}Fe^{3+}$ uptake. $^{55}FeCl_3$ was obtained from Perkin Elmer Life and Analytical Sciences (Billerica, MA, USA), in solution, at a concentration of 71.1 mM, with a specific activity of 10.18 Ci/g. Siderophore-^{55}Fe complexes were prepared at ^{55}Fe concentrations of 20 µM, with a siderophore: $^{55}Fe^{3+}$ (mol:mol) ratio of 20:1. **$^{55}Fe^{3+}$** uptake assays were carried out as previously described,[43] except that, after growth, bacteria were incubated with 0.2 µM PCH-^{55}Fe and with or without 0.2 and 2 µM PCH-Co or PCH-Zn complexes.

Electrophoresis mobility shift assays (EMSA). EMSA experiments were performed as previously described[44] using a DNA fragment gcgCGCCCGCCAATGATAATAAATCTCATTTCCCAACAgcg containing the -65 to -31 *pchD* promoter region containing a Fur box (underlined) with gcg on both side added for stabilization. DNA radiolabelling was performed by incubating 20-30 nM DNA for 30 min at 37°C in the presence of 1 unit T4 polynucleotide kinase (NEB) and 0.5 µL gamma ATP at 1 mCi /mmol. Labelled DNA was diluted 10 times in binding buffer (20 mM BisTrisPropane pH 8.5, 100 mM KCl, 3 mM $MgCl_2$, 10 µM $CoCl_2$, 5% v/v glycerol, and 0.01% Triton X-100), desalted on G25 mini-spin columns and stored at -20°C. EMSA were performed with 200-250 pM of freshly prepared radiolabelled DNA incubated 30 min at 25°C with various concentrations of Fur protein in binding buffer in the presence of 10 µM Co^{2+} or Mn^{2+}. Fur protein was purified as previously described.[44] After a 30-min incubation at room

temperature, 10 µL of each sample were loaded on an 8 % polyacrylamide (29/1) gel in TA buffer (40 mM Tris acetate pH 8.2) with 10 % glycerol, supplemented with 100 µM of $CoCl_2$. The gel was pre-run 30 min at 100 V in TA buffer supplemented with 100 µM of $CoCl_2$. Mobility shifts were revealed by exposing the gels (2 to 12 h at room remperature) on a storage phosphor screen (GE healthcare) and quantified with a cyclone phosphoimager (Perkin Elmer).

Transcriptional reporters. For the construction of transcriptional reporter plasmid pAYC5 (carrying both PchR and Fur boxes of *pchD* promoter), the promoters of the gene of interest were amplified from the chromosomal DNA of *P. aeruginosa* PAO1 by PCR with specific primers (Table SM2 in Supplemental Materials), allowing overlapping with a second PCR fragment encompassing the open reading frame of mCherry. A second PCR was performed using the two first PCR fragment as template to obtain the transcriptional reporter fragment. This fragment was trimmed by digestion with *Eco*RI and *Hind*III or *Bam*HI and inserted between the sites for these enzymes in pSEVA631 vector to generate pAYC5 and bacteria were transformed with this vector. The mutation of the Fur box of the *pch*D promoters to generate pAYC5-FURmut vector has been obtained with the Q5-site directed mutagenesis kit from New England Biolabs, using specific primers (Table 2SM).

Binding assays with MBP-PchR. The *E. coli* DH5α-pME7180 strain (Table 1), expressing the recombinant protein PchR tagged with MBP at the N-terminal domain,[45] was used to express MBP-PchR protein for the binding assays. The protein was purified (Figure SM3) as described previously[45] and the protocol from Lin *et al.*[46] was used to investigate the binding between MBP-PchR and the different PCH-metal complexes, metals, and apo-PCH. The PCH-metal complexes were generated by mixing 20 mM PCH with $FeCl_3$, $CoCl_2$, $NiCl_2$, or $ZnCl_2$ in methanol at a molar ratio of 2:1 (PCH:metal) to obtain a final metal concentration of 500 µM. The complexes were incubated for 15 min at RT and finally 50 mM Tris-HCl pH 8 was added to adjust the volume to the desired concentration. The complexes were prepared just before use for the binding experiments.

Quantitative real-time PCR. Specific gene expression was measured by RT-qPCR, as previously described.[47] Briefly, overnight cultures of strains grown in CAA medium were pelleted, re-suspended and diluted in fresh medium to obtain an OD_{600nm} of 0.1 units. The cells were then incubated in the presence or absence of 5 µM Fe^{3+} or Co^{2+}, with vigorous shaking, at 30°C for 8 h. RNAs were purified as described previously.[37] We then reverse transcribed 1 µg of total RNA with a High-Capacity RNAto-cDNA Kit, in accordance with the manufacturer's instructions (Applied Biosystems). The amounts of specific complementary DNAs were assessed in a StepOne Plus instrument (Applied Biosystems) with Power Sybr Green PCR Master Mix (Applied Biosystems) and the appropriate primers (Table SM2). The transcript levels for a given gene in a given strain were normalized with respect to those for *uvr*D and are expressed as a ratio (fold change) relative to the reference conditions.

Results

Co^{2+} can repress PCH and PVD production. We first investigated the impact of the biological metals (Co^{2+}, Cu^{2+}, Ni^{2+}, Mn^{2+} and Zn^{2+}) on the production of both siderophores PVD and PCH in iron restricted growth conditions. Bacteria were grown in casamino acids (CAA) medium in the presence of three metal concentrations (Figure 2). CAA contains approximately 20 nM Fe (LB Broth medium contains 4.3 µM)[13] and is considered to be highly iron-restricted. As previously described by Cunrath *et al.,*[13] PAO1 cells produced twice as much PVD as PCH under such growth conditions and in the absence of any biological metal: 116.5 ± 30.7 µM/$OD_{600\ nm}$ and 51.7 ± 3.1 µM/$OD_{600\ nm}$ for PVD and PCH, respectively.

The presence of Fe^{3+} completely repressed PVD production at 1 µM and PCH production only at 15 µM (Figure 2). Co^{2+} was the only other metal able to repress the production of both siderophores, with 41.1%, 48.5%, and 61.4% repression of PVD production in the presence of 1.5, 15, and 150 µM Co^{2+}, respectively. Surprisingly, we observed similar dose-dependent repression for both Fe^{3+} and Co^{2+} for PCH production. Ni^{2+} had no effect on PVD production and only affected PCH biosynthesis at 150 µM, repressing production by 42 %. Mn^{2+} and Zn^{2+} had no significant effect on either PVD or PCH production at the concentrations tested.

Overall, PVD production was repressed, as expected, by the presence of Fe^{3+}, but also to a lesser extent by Co^{2+}, whereas surprisingly PCH production was repressed with equivalent efficiency by Fe^{3+} and Co^{2+} and, to a lesser extent, by the presence of Ni^{2+}.

Genes up- and downregulated in P. aeruginosa cells in the presence of Co^{2+}. We further investigated the impact of the presence of Co^{2+} on *P. aeruginosa* by carrying out proteomic and transcriptomic analyses of bacteria grown in CAA medium with or without 10 µM Fe^{3+} or Co^{2+}. Changes in gene transcription and expression are given as the log2 ratio between *P. aeruginosa* grown with or without Co^{2+} (Table 2). The transcription and expression of several proteins of the PCH pathway was repressed in the presence of Fe^{3+} and Co^{2+}, showing a similar repressive effect of both metals, consistent with

the observed decrease of PCH production (Figure 2). In contrast, the transcription and expression of all genes detected belonging to the PVD pathway were repressed in the presence of Fe^{3+}, as expected, but at a clearly lower level in the presence of Co^{2+}. These data were confirmed by RT-qPCR experiments using several genes: two genes of the PVD pathway (an enzyme involved in PVD biosynthesis *pvdJ* and the transcriptional regulator *pvdS*) and five genes of the PCH pathway (the transcriptional regulator *pchR*, the inner membrane permease *fptX*, the outer membrane transporter *fptA* and two enzymes involved in PCH biosynthesis *pchA* and *pchE*) and the housekeeping gene *uvrD,* which was used for normalization (Figure 3A). RT-qPCR demonstrated a large decrease in transcript levels for all genes of the PCH pathway in the presence of both Fe^{3+} and Co^{2+}, except for the gene encoding the transcriptional regulator *pchR*. Concerning the genes of the PVD pathway, a strong repression is observed for the two genes tested with Fe^{3+} and at a lower extend with Co^{2+}. For Ni^{2+} and Zn^{2+} no significant transcriptional repression of the seven genes tested was observed (Figure 3A), but in some case a very small increase of transcription.

In conclusion, the transcription and expression of the proteins of the PCH pathway (exception for PchR) are more strongly repressed in the presence of Co^{2+}, than the genes of the PVD pathway.

Co^{2+} differently affects the expression of the genes the PCH operons. The RT-qPCR experiment (Figure 3A) highlighted for all genes of the PCH pathway, except for the one corresponding to the transcriptional regulator *pchR*, a large decrease in transcript levels in the presence of Co^{2+} compared to growth conditions in the absence of metals, while the presence of Fe^{3+} repressed the transcription of all genes including *pchR*. This observation indicates that Co^{2+}, and not Fe^{3+}, affects differently the transcription of the genes of PCH operons. The genes of these four PCH genes belong to three different operons: *pchA* and *pchE* belong to the two operons coding for the enzymes involved in PCH biosynthesis *pchDCBA* and *pchEFGHI*, *fptX* to the PCH-Fe *fptABCX* operon, and *pchR* which is not in an operon with other genes (Scheme 1). Co^{2+} is apparently able to repress *fptABCX*, *pchDCBA* and *pchEFGHI* operons and not *pchR.*

To investigate further this observation, we followed the expression of the four proteins PchA, PchE, FptX and PchR of the PCH pathway during bacterial growth, in the presence of the biological metals, using four strains that express fluorescent fusion proteins between mCherry and PchA (*pchA-mCherry* strain*,* Table 1), PchE (*pchE-mcherry*), FptX (*fptX-mCherry*), and the transcriptional regulator PchR (*mCherry-pchR*).[48] These proteins were tagged with mCherry at the N- or C-terminal end, and the tagged proteins chromosomally integrated. The presence of the tag has been shown to affect neither the transcription of the proteins (by RT-qPCR) nor their biological activities (siderophore production or ferri-siderophore uptake).[48] During bacterial growth, in the absence of any metals, two different variation of mCHERRY fluorescence were observed depending on the strains. For *pchA-mCherry, pchE-mcherry* and *fptX-mCherry* strains a strong increase of fluorescence is observed corresponding to an increase of PchA-mCHERRY, PchE-mCHERRY and FptX-mCHERRY fusion protein expression (Figure 3B). On the opposite, for *mcherry-pchR* in the same growth conditions, mCHERRY fluorescence decreased slightly after 6 hours culture (Figure 3C). As expected, the presence of 5 µM Fe^{3+} repressed strongly PchA-mCHERRY, PchE-mCHERRY, mCHERRY-FptX and mCHERRY-PchR fusion protein expression during bacterial growth. Consistent with the RT-qPCR data (Figure 3A), Co^{2+} repressed the expression of PchA-mCHERRY, PchE-mCHERRY and mCHERRY-FptX but not of mCHERRY-PchR. Ni^{2+} and Zn^{2+} at the concentrations tested had no effect on the expression of the four fusion proteins. Actually their presence slightly induced the expression of PchA-mCHERRY, PchE-mCHERRY and mCHERRY-FptX, probably because of the metal-restriction growth conditions.

Based on the *P. aeruginosa* genome, *pchR* expression is regulated solely by Fur (presence only of a Fur-Box) and *pchDCBA*, *pchEFGHI*, and *fptABCX* operons by both Fur and PchR regulators (the presence of both Fur- and PchR-boxes upstream of these genes) (Scheme 1). Our data show that the presence of Co^{2+} inhibits only the transcription of genes that depend on a PchR box for their expression.

Co^{2+} can enter P. aeruginosa cells by the TonB-dependent transporter FptA. According to current knowledge concerning the interaction of the transcriptional regulators Fur and PchR with Fe (formation of Fur-Fe and PchR-PCH-Fe complexes), the interaction of Co^{2+} with one of these regulators includes the importation of Co^{2+} into the bacteria and, in the case of PchR, the presence of PCH-Co to form a PchR-PCH-Co complex.[46] When Co^{2+}, Ni^{2+} and Zn^{2+} are incubated with PCH in solution, the UV spectral modifications observed compared to the UV spectrum of apo PCH, indicates that PCH is able to chelate these three metals (Figure 2SM). Moreover, previously we have determined a Ka of PCH for Zn^{2+} of Ka = $10^{26.0}$ M^{-2} (Ka = $10^{28.8}$ M^{-2} for Fe^{3+}).[28] Previous studies of our group, in which we used ICP-AES (Inductively Coupled Plasma Atomic Emission Spectroscopy, which allows the detection of metals traces), showed that Co^{2+} and Ni^{2+} can both enter *P. aeruginosa* cells *via* the FptA/PCH pathway when bacteria were grown in succinate-containing medium.[24] Here, we used the same approach to verify that bacteria grown in CAA medium are also able to efficiently import Co^{2+} and Ni^{2+}. CAA is 10 fold more iron-restricted than succinate medium: iron concentration of 300 nM for succinate medium and 20 nM for CAA.[13] We used a PVD and PCH-deficient strain (Δ*pvdF*Δ*pchA*, Table 1) to control the presence of siderophores and their concentrations in the assay. The importance of the PCH pathway in metal uptake was evaluated by using the *fptA* (PCH-Fe outer membrane transporter) mutant strain *ΔpvdFΔpchAΔfptA* (Table 1).

As expected, *fptA* deletion markedly affected Fe accumulation in *P. aeruginosa* cells in the presence of PCH (Figure 4A), as well as that of Co^{2+}, showing that Co^{2+} is imported into *P. aeruginosa* cells by the FptA transporter (Figure 4A). Co^{2+} uptake certainly occurs in a complex with PCH, since this transporter recognizes only PCH-metal complexes and not siderophore-free metals.[49,50] However, the amount of Co^{2+} imported by the FptA/Pch system is lower than the amount of Fe^{3+} acquired. We observed no significant FptA-dependent uptake for Ni^{2+} and Zn^{2+} at the metal concentrations tested here, as previously reported.[24]

We also investigated the ability of PCH-Co complexes to compete with and inhibit PCH-^{55}Fe import in *P. aeruginosa* cells. The PVD and PCH-deficient strain (Δ*pvdF*Δ*pchA*) was incubated with 0.2 µM PCH-

^{55}Fe with or without 0.2 µM and 2 µM (1 and 10-fold excess) PCH-metal complexes and the radioactivity incorporated into the bacteria (during a 30-min incubation) counted. Incubation of the bacteria in the presence of PCH-^{55}Fe alone resulted in the uptake of approximately 90 pmol of ^{55}Fe per cell per 30 min (Figure 4B). We observed 60 % inhibition of this uptake in the presence of 2 µM PCH-Co. We also carried out a competition assay with PCH-Ni and PCH-Zn complexes, but observed no significant inhibition of ^{55}Fe uptake *via* PCH.

These data all suggest that, in the range of metal concentrations tested, Co^{2+} and Ni^{2+} can enter bacteria both by diffusion (Co^{2+} and Ni^{2+} accumulation in the *fptA* mutant, Figure 3A) and also *via* the PCH/FptA uptake system for Co^{2+}. Consequently, PCH-Co complexes, as well as siderophore-free Co^{2+} and Ni^{2+}, are present in *P. aeruginosa* cells.

The presence of Co^{2+} in the bacterial environment does not affect the intracellular iron concentration in P. aeruginosa cells. *P. aeruginosa* PAO1 cells were also grown in the presence of 5 µM Co^{2+} or Ni^{2+} to assess how the intracellular concentrations of all biological metals were affected by the presence of an excess of these two metals (Figure 5). Surprisingly, although Co^{2+} can enter bacteria by diffusion or in competition with Fe^{3+} by the FptA/PCH pathway, the intracellular iron concentration was not affected. This suggests that bacteria can adapt to potential competition between Fe^{3+} and Co^{2+} for the FptA/PCH system during growth and that the intracellular iron content is maintained, even in the presence of 5 µM Co^{2+} contamination.

Excess Co^{2+} in the bacterial environment does not affect Fur regulation. We next elucidated the molecular mechanism involved in the Co-dependent repression of PCH pathway expression by investigating the ability of Fur-Co complexes to interact with the Fur boxes *in vitro*. *E. coli* Fur has been shown to bind DNA sequences containing Fur boxes by interacting with metals other than Fe^{2+} [51] and Fur of *P. aeruginosa* has been shown to be capable of binding to the Fur box in the presence of Co^{2+} in a nuclease protection assay[44] and in the presence of Mn^{2+} in an EMSA (electrophoretic mobility shift

assay) assay.[52] It is not possible to run EMSA in the presence of Fe^{2+} because of its oxidation. Consequently, it is well accepted in the literature to use Mn^{2+} ions to mimic Fe^{2+} for the DNA binding assay.[52] Here EMSA experiments were carried out in the presence of Co^{2+} and Mn^{2+}, with purified Fur protein and the promoter region of *pchD*, containing the Fur-box present upstream of the *pchDCBE* operon. An interaction between Fur-Co and the *pchD* promoter sequence was observed (Figure 6), proving that Fur-Co is able to bind to this sequence. However, our proteomic, transcriptomic and RT-qPCR data (Table 2 and Figure 3A), as well as the expression data using mCherry fusion proteins (Figure 3B-3C), clearly show that the presence of Co^{2+} in the bacterial environment does not repress all Fur-dependent genes, as does the presence of Fe^{3+}. Therefore, we also used a plasmid (pAYC5) carrying the mCherry sequence and the PCH promoter of *pchDCBA* operon (Table 1SM) to investigate the behavior of Fur in the presence of Co^{2+} in *P. aeruginosa* cells. Since this promoter region also contains a PchR box, we carried out this experiments in strain unable to express PchR (Δ*pchR* strain). Bacteria carrying this construct were grown in CAA medium with increasing concentration (0-100 µM) of Co^{2+} or Fe^{3+} and the mCherry fluorescent signal monitored at 610 nm (excitation at 570 nm). As expected, the addition of Fe^{3+} to the bacterial growth medium caused the repression of mCherry expression (Figure 7A): the Fur-Fe complex interacts with the bacterial Fur boxes, which represses the transcription and expression of mCherry and any Fur-dependent genes. The addition of Co^{2+} to the bacterial medium had no significant effect on mCherry expression (Figure 7B) for concentrations of Co^{2+} equivalent or lower than 10 µM and a weak effect was observed at 100 µM. We carried out the same experiment with 10 and 100 µM Ni^{2+} or Zn^{2+} (Figure 7C and 7D) and no repression of mCherry expression was observed.

Overall, our data show that, Fur-Co can bind to the PCH Fur-box but does not repress Fur-dependent gene expression *in vivo* like Fe^{2+} whereas equivalent effects are observed for both metals for PCH production (Figure 2).

The purified cytoplasmic regulator PchR can bind to PCH-Co and PCH-Ni in addition to PCH-Fe. PchR,

the transcriptional activator of the genes of the PCH pathway, activates the transcription of all PCH genes, except *pchR*, by interacting with the PchR box (no PchR box upstream of *pchR* gene).[21–23] We carried out binding assays between purified PchR (MBP fused PchR[46] and purified protein shown in Figure SM3) and PCH-Co and PCH-Ni, based on a spectroscopy approach previously described, using the fluorescent properties of the tryptophans (Trp) of PchR published previously.[46] When MBP-PchR is excited at 280 nm, tryptophan present in the protein emits intrinsic fluorescence with maximal intensity at 330 nm (Figure 4SM). Upon the addition of ligands, such as PCH-Fe, the fluorescence is quenched. Thus, the protein's affinity for its ligand can be determined by plotting the relative fluorescence intensity, F_0/F, with F_0 being the fluorescence emitted by MBP-PchR without ligand and F the fluorescence emitted by MBP-PchR once a specific concentration of ligand has been added. Afterwards, K_d values are determined using the Stern-Volmer representation and linear regression. PCH-metal complexes were prepared by incubating 2 equivalent of PCH with one of metal (Figure 2SM).

We determined an affinity of PCH-Fe (K_d = 5.82 ± 2.84 µM) for MBP-PchR that was slightly better as that described previously (K_d = 41 ± 5 µM)[46]. PCH-Co was also able to bind to PchR with a K_d of 13.9 ± 3.4 µM, as well as PCH-Ni and PCH-Zn (Kd values of 42 ± 4.3 µM and 47.4 ± 2.2 µM, respectively -for details see Figure 4SM). We were unable to investigate the ability of PchR-PCH-Co to bind the PchR box (EMSA assays with the purified MBP fused PchR protein), probably because of the presence of the tag, as well as problems with protein aggregation.

Role of PchR in the repression of the PCH pathway in the presence of Co^{2+} and Ni^{2+}. We further explored the mechanism involved in the repression of PCH production observed in the presence of Co^{2+} and Ni^{2+} by constructing a plasmid (pAYC5-FURmut) carrying the mCherry sequence and the promoter of the *pchDCBA* operon containing only the PchR box and the Fur box having being mutated (Table 1SM and 2SM). The strains PAO1 and Δ*pchR* (unable to express PchR) carrying this plasmid were grown in CAA medium supplemented with increasing concentrations of metals (Fe^{2+}, Co^{2+}, Ni^{2+}

or Zn^{2+}). In the absence of metals, in the WT (PAO1) background (kinetics with black dots in Figure 8A-8D), the fluorescence corresponding to mCherry expression highly increased in function of time, but not in the Δ*pchR* strain unable to express the transcriptional activator PchR (kinetics with grey triangles in Figure 8A-8D), indicating that PchR is necessary to observe mCherry expression. For PAO1, in the presence of increasing concentrations of Fe^{3+}, this fluorescence corresponding to mCherry expression decreased during bacterial growth (Figure 8A). This observation is due to Fur which gets loaded with Fe^{2+}, interacts with its promoter regions and consequently the expression of PchR and the other proteins of the PCH pathway is repressed (Figure 3A and Table 2). Since less PchR is expressed, *mcherry* transcription is no more activated and lower level of fluorescence are observed compared to the condition in the absence of metal.

In the presence of increasing concentrations of Co^{2+} or Ni^{2+} (but not Zn^{2+}; Figure 8B-8D), the fluorescence corresponding to mCherry expression also decreased in PAO1 cultures, but less than in the presence of Fe^{3+}. Higher concentrations of Co^{2+} (10 µM) and Ni^{2+} (100 µM) are necessary to elicit an effect equivalent to that observed with Fe^{3+} (5 µM). In that case, the decrease of fluorescence is not due to an absence of PchR expression, since Co^{2+} or Ni^{2+} present in the *P. aeruginosa* environment were both unable to repress the expression of Fur-regulated genes (Figure 7). Co^{2+} (and probably also Ni^{2+}) are likely present in the bacterial cytoplasm, mostly in their PCH-complexed forms (50 µM is the concentration of PCH in the bacterial culture and 5 µM metals are added to the growth media). Increasing concentrations of PCH-Co or PCH-Ni complexes in the bacterial cytoplasm certainly leads to an increase in the concentrations of PchR-PCH-Co or PchR-PCH-Ni complexes, at the expense of PchR-PCH-Fe complexes, but only PchR-PCH-Fe complexes are probably able to activate transcription of the genes for the proteins of the PCH pathway and *mcherry* from pAYC5-FURmut plasmid. In such a scenario, the expression of PchR-regulated genes, as the genes of the PCH pathway, is less highly activated and less PCH is produced (Figure 2). This also explains why the presence of Co^{2+} or Ni^{2+} does not repress *pchR* expression, as the transcription of this gene is not regulated by the PchR promoter, but only the Fur box (Scheme 1).[45]

In conclusion, the presence of high levels of Fe^{3+}, Co^{2+}, or Ni^{2+} (to a lesser extent) in the bacterial environment induces repression of the transcription of PCH genes (except *pchR*) by two different molecular mechanisms. In the presence of Fe^{3+} in the bacterial environment, the transcriptional repressor Fur, in a complex with Fe^{2+}, represses the expression of these genes. In the presence of Co^{2+} or Ni^{2+}, Fur is not involved, but rather the transcriptional activator PchR, which is no more able to activate the production of PCH, probably due to a decrease in the intracellular concentration of PchR-PCH-Fe complexes.

Discussion

The requirement for different biological metals in bacteria are very different and depend on their biological function. The relative intracellular concentrations of these metals in *P. aeruginosa* PAO1 cells are Na-K > Mg >> Ca >> Fe-Zn >> Mn-Mo-Cu-V-Cr-Ni >> Co[13], with Fe and Zn being the two most abundant transition metals (concentrations between 10^{-3} and 10^{-4} M, depending on the growth medium). The intracellular concentrations of Cu, Mn, Mo, and Ni are generally between 10^{-5} and 10^{-4} M[13] and Co is used only in very small amounts by *P. aeruginosa* (a concentration too low to be detected by ICP-AES[13]). Very similar values have been described for wild type *E. coli*[53] and can probably be found in many Gram-negative bacteria in planktonic growth conditions.

Since, all biological metals become toxic at high concentrations and are highly deleterious to living organisms, the intracellular concentrations of these biological metals have to be finely regulated to stay constant. Siderophores play a key role in iron homeostasis.[21] Increasing number of publications also suggest that siderophores may play a role in the homeostasis of other biological metals.[18] Indeed, these compounds are able to chelate many metals other than Fe^{3+},[18] their production can be modulated by different metals[30–34] and they often play a role in bacterial metal resistance.[17,18] These observations lead to the question whether bacteria are able to activate their siderophore production in response to the presence of metals other than Fe^{3+}. As in previous studies,[24] we showed that none of the metals tested was able to significantly activate PVD or PCH production above that induced by iron restriction (Figure 2). Moreover, there is currently no data available to support the existence of bacterial sensors that detect toxic metals in the bacterial environment and consequently activate siderophore production. All current data suggest that for example the protective role of siderophores against toxic metals is probably only a consequence of the presence of large amounts of siderophores produced in response to iron starvation. However, the formation of siderophore-metal complexes with metals other than Fe^{3+} may increase the sense of iron starvation by bacteria, because siderophores are in complex with metals other than Fe^{3+} and consequently less siderophore-Fe is imported into the bacteria.

In the present work, Co^{2+} and Ni^{2+} were able to repress the production of PCH and for Co^{2+}, with the same efficiency as Fe^{3+}. PCH production is positively regulated by the transcriptional activator PchR and negatively by the transcriptional repressor Fur (Scheme 1). PchR activates the transcription of all PCH genes, except *pchR*, by interacting with the PchR box (no PchR box upstream of *pchR*, Scheme 1). Consequently, a decrease of PCH production must be due to either Fur-dependent repression or the inability of PchR to still activate PCH production. Our data show that Fur regulation is insensitive to the presence of excess Co^{2+} (or Ni^{2+}), even if Co^{2+} bound to Fur proteins *in vitro* and formed complexes with Fur boxes. Our experimental data show that the repression of PCH production by Co^{2+} and Ni^{2+} involves PchR. They also show that PCH-Co enters bacteria via the TonB-dependent outer membrane transporter FptA and can bind to PchR *in vitro*. Since a repression of PCH production is as well observed in the presence of Ni^{2+}, we cannot exclude that PCH-Ni is also able to enter *P. aeruginosa* cells but with uptake rates too low to be detected by our approach. Altogether, these data describe a mechanism in which PCH-Co, after entering *P. aeruginosa* cells by FptA, interacts with PchR to form PchR-PCH-Co complexes unable to activate the transcription of PchR-regulated genes. The formation of PchR-PCH-Co or PchR-PCH-Ni complexes in the bacterial cytoplasm certainly leads to a decrease in the intracellular concentration of PchR-PCH-Fe, leading to a decrease in the transcription of PCH pathway genes and, thus, the production of PCH.

The repression of PCH production was more pronounced with Co^{2+} than Ni^{2+} and cannot be explained simply by the difference in affinities of PchR for the PCH-Co and PCH-Ni complexes. Previous studies, based on titration experiments, have shown that the binding affinity of PCH is higher for Ni^{2+} than Co^{2+} (relative affinity of PCH for biological metals having been proposed Fe(III) > Mo(VI) = Cu(II) > Ni(II) > Co(II) > Zn(II) > Mn(II).[33] On the contrary, the PCH-Co complex more efficiently competes with PCH-Fe for the TonB-dependent transporter FptA (affinities of PCH-Co and PCH-Ni for FptA in the range of 15 nM and 50 nM, respectively[24]) and is more efficiently transported into *P. aeruginosa* cells. The higher efficiency of Co^{2+} to repress PCH production is probably linked to its higher ability to enter *P. aeruginosa* cells as a PCH-Co complex relative to PCH-Ni.

ICP-AES measurements of intracellular metal concentrations of *P. aeruginosa* cells grown with or without Co^{2+} showed no effect of this metal on the intracellular iron concentration. This indicates that the inhibition of PCH production in the presence of Co^{2+} has little effect on bacterial iron homeostasis under our growth conditions. The ability of Co^{2+} to interfere with Fe^{3+} acquisition *via* the PCH/FptA pathway (55 % inhibition of PCH-^{55}Fe uptake in *P. aeruginosa* PAO1 cells when incubated for 30 min in the presence of PCH-Co complexes) does not affect the access to iron of the pathogen. This organism uses several strategies to obtain access to iron; if one iron acquisition pathway is compromised, the bacteria simply uses another.[12]

FptA plays a key role in the outer membrane for the uptake of the right metal by PCH. Previous studies from our group have shown that FptA at the bacterial surface can bind different PCH-metal complexes, with affinities ranging from 10 nM to 4.8 µM, (the affinity of PCH-Fe being 10 nM).[24] However, only Fe^{3+} and, to a lesser extent, Co^{2+} can accumulate significantly in *P. aeruginosa* cells via the PCH pathway, but with uptake rates clearly lower than those for Fe^{3+}. Moreover, previous studies have also shown that PCH complexes Ga^{3+} and the formed complex is transported into *P. aeruginosa* cells via FptA.[24,54] Ni^{2+} is probably also transported in complex with PCH with low uptake rates, since the presence of this metal in the bacterial environment represses PchR regulated genes. FptA, due to its uptake specificity, avoids and controls the uptake of most metals other than Fe^{3+} across the outer membrane and limits the uptake of Co^{2+} and Ni^{2+}. Fe^{3+}, Co^{2+} and Ni^{2+} are part of the iron triad and all three elements show similar properties such as the metallic radius (124, 125, 125 pm, respectively) and the electronic configuration. Ga^{3+} has a radius slightly larger (187 ppm) than Fe^{3+} but very similar coordination properties. Consequently, PCH-Co, PCH-Ni and PCH-Ga have certainly very close conformations, which is not the case for PCH-Cu and PCH-Zn complexes (two metals with different coordination properties compared to Fe^{3+}). The metallic radius and similar coordination properties could be responsible for the high specificity of FptA for PCH-metal complexes.

We are aware that the µM concentrations of Co^{2+} and Ni^{2+} used in this study are not truly physiological in the natural environment thrived by *P. aeruginosa,* and exposure to such concentrations appears unlike during infections and exceptional also in natural environment. However, such concentrations are often used in the literature in studies investigating the role of siderophores in bacterial resistance to metals or in development of bioremediation processes using siderophore producing bacteria to decontaminated metal polluted media or wastes. In such contexts, it is important to understand how siderophore production and siderophore-dependent Fe^{3+} uptake pathways in bacteria interfere with an excess of metals other than Fe^{3+} and what are the molecular mechanisms involved.

Conclusion

We show for the first time, how an excess of biological metals, other than iron, can interfere with transcriptional regulators that control the transcription of genes of the PCH pathway. The presence of high levels of Fe^{3+}, Co^{2+}, or Ni^{2+} (to a lesser extent) in the bacterial environment represses the transcription of PCH genes by two different molecular mechanisms. In the presence of increasing Fe^{3+} concentrations, the transcriptional repressor Fur gets loaded with Fe^{2+} and represses the expression of all *pch* genes. In the presence of increasing Co^{2+} or Ni^{2+} concentrations, Fur is not involved, but the transcriptional activator PchR gets loaded with PCH-Co and PCH-Ni and consequently is no more able to activate the transcription of *pch* genes, due to a decrease in the intracellular concentration of PchR-PCH-Fe complexes.

PchR appears to have broad metal-binding specificity, but since only a few metals (Fe^{3+}, Ga^{3+}, Co^{2+}, and Ni^{2+}) are able to enter bacteria by the FptA/PCH pathway, most which could be present as a contaminant in the bacterial environment do not affect PCH production. Indeed, FptA acts as a selective gate for the uptake of PCH-metal complexes and allows the uptake of only PCH-Fe and, to a lesser extent, PCH-Ga, PCH-Co, and PCH-Ni. The presence of these PCH-metal complexes in the bacterial cytoplasm interferes with the regulation of PCH production by interacting with PchR and inhibiting the positive autoregulatory loop that involves PchR (Scheme 2). The inability of PchR-PCH-

Co and PchR-PCH-Ni to activate the expression of PCH genes highly suggests that PCH is not involved in the acquisition by *P. aeruginosa* of these two metals, but that their uptake via PCH is simply a non-specific interference of these two metals with the PCH pathway. Moreover, the Achilles heel of the *P. aeruginosa* PCH pathway, in terms of excess Co^{2+} in the bacterial environment, is the selectivity of FptA for metal transport. However, the ability of PchR to interact with many different PCH-metal complexes leads to a decrease in PCH production and consequently a decrease in PCH-Co and PCH-Ni import.

Conflicts of interest

There are no conflicts to declare.

Acknowledgments

This work was partly funded by the *Centre National de la Recherche Scientifique*. O. Cunrath held a fellowship from the French *Ministère de la Recherche et de la Technologie* (3 years) and the FRM (*Fondation pour la Recherche Médical*, 6 months). A.Y Carballido Lopez held a fellowship from the University of Strasbourg (IDEX) and B. Pesset from the DGA (Direction Générale des l'Armement). J.P. and I.M.S. thank the Laboratory of Excellence GRAL (grant ANR-11-LABX-49-01) and the Labex ARCANE (grant ANR-11-LABX-0003-01). The Transcriptome and Epigenome Platform is a member of the France Génomique consortium (ANR10-NBS-09-08). We thank Dr A. Boos and P. Ronot (Institut Pluridisciplinaire Hubert Curien, Strasbourg) for their help in the ICP-AES measurements.

Author contributions

ACL evaluated the siderophore production in the presence of metals, performed the iron uptake assays, the experiment with the fluorescent strains (Figure 2) and binding assays with MBP-PchR. OC performed the metal uptake assays and metal quantifications. AF realized the molecular biology

(plasmid and strain constructions) and the fluorescent experiments in Figure 7 with GG. RL, HV, OS, JYC performed the transcriptional experiments and analyses. PMS and DB performed the proteomic experiments and analysis. JP and IM-S performed the electrophoresis mobility shift assays. BP and GLAM synthesized the PCH used in the experiments. QP realized the spectral characterization of PCH-metal complexes. PF realized the RT-qPCR experiment and participated in the design of all experiments and the analysis of all data. IJS directed the project, analyzed data and wrote the paper. All authors discussed the results and contributed to the writing of the manuscript.

References

1 C. L. Dupont, S. Yang, B. Palenik and P. E. Bourne, *Proc. Natl. Acad. Sci. U. S. A.*, 2006, **103**, 17822–17827.
2 N. J. Robinson, *Nat Chem Biol*, 2007, **3**, 692–3.
3 K. J. Waldron, J. C. Rutherford, D. Ford and N. J. Robinson, *Nature*, 2009, **460**, 823–30.
4 E. D. Weinberg, *Biochim. Biophys. Acta*, 2009, **1790**, 600–605.
5 T. E. Kehl-Fie and E. P. Skaar, *Curr. Opin. Chem. Biol.*, 2010, **14**, 218–224.
6 K. Y. Djoko, C. Y. Ong, M. J. Walker and A. G. McEwan, *J. Biol. Chem.*, 2015, **290**, 18954–18961.
7 R. C. Hider and X. Kong, *Nat Prod Rep*, 2011, **27**, 637–57.
8 K. N. Raymond, E. A. Dertz and S. S. Kim, *Proc Natl Acad Sci U A*, 2003, **100**, 3584–8.
9 P. Cornelis, *Appl Microbiol Biotechnol*, 2010, **86**, 1637–45.
10 I. J. Schalk and L. Guillon, *Amino Acids*, 2013, **44**, 1267–1277.
11 P. E. Powell, G. R. Cline, C. P. P. Reid and P. J. Szaniszlo, *Nature*, 1980, **287**, 833–834.
12 P. Cornelis and J. Dingemans, *Front Cell Infect Microbiol*, 2013, **3**, 75.
13 O. Cunrath, V. A. Geoffroy and I. J. Schalk, *Environ. Microbiol.*, 2016, **18**, 3258–3267.
14 Z. Dumas, A. Ross-Gillespie and R. Kümmerli, *Proc. Biol. Sci.*, 2013, **280**, 20131055.
15 I. J. Schalk, G. L. A. Mislin and K. Brillet, *Curr. Top. Membr.*, 2012, **69**, 37–66.
16 I. J. Schalk and L. Guillon, *Environ. Microbiol.*, 2013, **15**, 1661–1673.
17 A. Braud, V. Geoffroy, F. Hoegy, G. L. A. Mislin and I. J. Schalk, *Env. Microbiol Rep.*, 2010, **2**, 419–425.
18 I. J. Schalk, M. Hannauer and A. Braud, *Env. Microbiol*, 2011, **13**, 2844–54.
19 M. F. Fillat, *Arch. Biochem. Biophys.*, 2014, **546**, 41–52.
20 M. A. Llamas, F. Imperi, P. Visca and I. L. Lamont, *FEMS Microbiol Rev*, 2014, **38**, 569–97.
21 P. Cornelis, S. Matthijs and L. Van Oeffelen, *Biometals*, 2009, **22**, 15–22.
22 P. Visca, *Pseudomonas Vol. 2 Ed. Juan-Luis Ramos Kluver Acad. Publ. New-York*, 2004, 69–123.
23 Z. A. Youard and C. Reimmann, *Microbiol. Read. Engl.*, 2010, **156**, 1772–1782.
24 A. Braud, M. Hannauer, G. L. A. Mislin and I. J. Schalk, *J Bacteriol*, 2009, **191**, 5317–25.
25 A. Braud, F. Hoegy, K. Jezequel, T. Lebeau and I. J. Schalk, *Env. Microbiol*, 2009, **11**, 1079–91.
26 A. M. Albrecht-Gary, S. Blanc, N. Rochel, A. Z. Ocacktan and M. A. Abdallah, *Inorg Chem*, 1994, **33**, 6391–6402.

27 C. Ferret, J. Y. Cornu, M. Elhabiri, T. Sterckeman, A. Braud, K. Jezequel, M. Lollier, T. Lebeau, I. J. Schalk and V. A. Geoffroy, *Env. Sci Pollut Res Int*, , DOI:10.1007/s11356-014-3487-2.
28 J. Brandel, N. Humbert, M. Elhabiri, I. J. Schalk, G. L. A. Mislin and A.-M. Albrecht-Garry, *Dalton Trans*, 2012, **41**, 2820–34.
29 C. Baysse, D. De Vos, Y. Naudet, A. Vandermonde, U. Ochsner, J. M. Meyer, H. Budzikiewicz, M. Schafer, R. Fuchs and P. Cornelis, *Microbiology*, 2000, **146 (Pt 10)**, 2425–34.
30 M. Huyer and W. J. Page, *Appl Env. Microbiol*, 1988, **54**, 2625–2631.
31 M. Hofte, S. Buysens, N. Koedam and P. Cornelis, *Biometals*, 1993, **6**, 85–91.
32 X. Hu and G. L. Boyer, *Appl Env. Microbiol*, 1996, **62**, 4044–4048.
33 P. Visca, G. Colotti, L. Serino, D. Verzili, N. Orsi and E. Chiancone, *Appl Env. Microbiol*, 1992, **58**, 2886–93.
34 G. M. Teitzel, A. Geddie, S. K. De Long, M. J. Kirisits, M. Whiteley and M. R. Parsek, *J Bacteriol*, 2006, **188**, 7242–56.
35 A. Zamri and M. A. Abdallah, *Tetrahedron*, 2000, **56**, 249–256.
36 F. Hoegy, G. L. Mislin and I. J. Schalk, *Methods Mol Biol*, 2014, **1149**, 293–301.
37 V. Gasser, E. Baco, O. Cunrath, P. S. August, Q. Perraud, N. Zill, C. Schleberger, A. Schmidt, A. Paulen, D. Bumann, G. L. A. Mislin and I. J. Schalk, *Environ. Microbiol.*, 2016, **18**, 819–832.
38 R Core Team, .
39 M. I. Love, W. Huber and S. Anders, *Genome Biol.*, 2014, **15**, 550.
40 Y. Benjamini and Y. Hochberg, *J. R. Stat. Soc.*, 1995, **57**, 289–300.
41 B. Langmead, C. Trapnell, M. Pop and S. L. Salzberg, *Genome Biol.*, 2009, **10**, R25.
42 Y. Liao, G. K. Smyth and W. Shi, *Bioinforma. Oxf. Engl.*, 2014, **30**, 923–930.
43 F. Hoegy and I. J. Schalk, *Methods Mol Biol*, 2014, **1149**, 337–46.
44 J. Pérard, J. Covès, M. Castellan, C. Solard, M. Savard, R. Miras, S. Galop, L. Signor, S. Crouzy, I. Michaud-Soret and E. de Rosny, *Biochemistry*, 2016, **55**, 1503–1515.
45 L. Michel, N. Gonzalez, S. Jagdeep, T. Nguyen-Ngoc and C. Reimmann, *Mol Microbiol*, 2005, **58**, 495–509.
46 P.-C. Lin, Z. A. Youard and C. Reimmann, *Biometals Int. J. Role Met. Ions Biol. Biochem. Med.*, 2013, **26**, 1067–1073.
47 H. Gross and J. E. Loper, *Nat Prod Rep*, 2009, **26**, 1408–46.
48 O. Cunrath, V. Gasser, F. Hoegy, C. Reimmann, L. Guillon and I. J. Schalk, *Env. Microbiol*, 2015, **17**, 171–85.
49 D. Cobessi, H. Celia, N. Folschweiller, M. Heymann, I. Schalk, M. Abdallah and F. Pattus, *Acta Crystallogr Biol Crystallogr*, 2004, **60**, 1467–9.
50 K. Brillet, C. Reimmann, G. L. A. Mislin, S. Noël, D. Rognan, I. J. Schalk and D. Cobessi, *J Am Chem Soc*, 2011, **133**, 16503–9.
51 A. Adrait, L. Jacquamet, L. Le Pape, A. Gonzalez de Peredo, D. Aberdam, J. L. Hazemann, J. M. Latour and I. Michaud-Soret, *Biochemistry*, 1999, **38**, 6248–6260.
52 U. A. Ochsner, A. I. Vasil and M. L. Vasil, *J Bacteriol*, 1995, **177**, 7194–201.
53 C. E. Outten and T. V. O'Halloran, *Science*, 2001, **292**, 2488–92.
54 E. Frangipani, C. Bonchi, F. Minandri, F. Imperi and P. Visca, *Antimicrob. Agents Chemother.*, 2014, **58**, 5572–5575.
55 C. K. Stover, X. Q. Pham, A. L. Erwin, S. D. Mizoguchi, P. Warrener, M. J. Hickey, F. S. Brinkman, W. O. Hufnagle, D. J. Kowalik, M. Lagrou, R. L. Garber, L. Goltry, E. Tolentino, S. Westbrock-Wadman, Y. Yuan, L. L. Brody, S. N. Coulter, K. R. Folger, A. Kas, K. Larbig, R. Lim, K. Smith, D. Spencer, G. K. Wong, Z. Wu, I. T. Paulsen, J. Reizer, M. H. Saier, R. E. Hancock, S. Lory and M. V. Olson, *Nature*, 2000, **406**, 959–64.
56 V. Gasser, L. Guillon, O. Cunrath and I. J. Schalk, *J Inorg Biochem*, 2015, **148**, 27–34.
57 E. Martínez-García, T. Aparicio, A. Goñi-Moreno, S. Fraile and V. de Lorenzo, *Nucleic Acids Res.*, 2015, **43**, D1183-1189.
58 L. Guillon, S. Altenburger, P. L. Graumann and I. J. Schalk, *PLoS ONE*, 2013, **8**, e79111.

Strains	Coll. Ref.	Description	Ref.
PAO1	PAS43	ATCC15692. *P. aeruginosa* wild-type strain	[55]
ΔpvdFΔpchAΔfptA	PAS273	Deletion of *pvdF*, *pchA* and *fptA* genes	[48]
ΔpvdFΔpchA	PAS283	Deletion of *pvdF* and *pchA* genes in PAO1	[48]
pchA-mCherry	PAS193	Derivate of PAO1 *wt*; *pchAmcherry* chromosomally integrated	[56]
pchE-mcherry	PAS195	Derivate of PAO1 *wt*; *pchEmcherry* chromosomally integrated	[48]
fptX-mCherry	PAS210	Derivate of PAO1 *wt*; *fptXmcherry* chromosomally integrated	[48]
mCherry-pchR	PAS208	Derivate of PAO1 *wt*; *mcherrypchR* chromosomally integrated	[48]
ΔpchR	PAS387	Deletion of *pchR* in PAO1	[48]
E. coli DH5α	-	Strain with pME7180 plasmid carrying *MBP* added to the *5'pchR* under the effect of the lac promoter induced by IPTG	[45]
E. coli HB101		Helper strain carrying pME487	Promega
E.coli Top10	-	F- mcrA Δ(mrr-hsdRMS-mcrBC) ϕ80lacZΔM15 ΔlacX74 nupG recA1 araD139 Δ(ara-leu)7697 galE15 galK16 rpsL(StrR) endA1 λ	Invitrogen
Plasmids			
pAYC5	pAYC5	*pchD* promoter containing the Fur box and PchR box fused to mCherry ORF	This study
pAYC5-FURmut	pAYC5-FURmut	*pchD* promoter containing the Fur mutated box and PchR box fused to mCherry ORF	This study
pSEVA631	244	Low copy plasmid for *E. coli / Pseudomonas spp.*	[57]
pLG3	154	Expression vector carrying mCherry sequence	[58]

Table 1. Bacterial strains and plasmids used in this study.

		Down regulated genes							
		PAO1							
		Fe^{3+}				Co^{2+}			
		Transcriptome		Proteome		Transcriptome		Proteome	
ID		log2 fc	p-value	log2 ratio	p-value	log2 fc	p-value	log2 ratio	p-value
PCH pathway									
PA4218	***fptX***	-7.5	<1.0E-300	-2.1	2.2E-02	-3.8	2.3e-297	-1.9	1.7E-02
PA4221	***fptA***	-7.9	<1.0E-300	-2.9	1.5E-04	-4.2	<1.0E-300	-3.2	1.0E-04
PA4222	***pchI***	-7.5	<1.0E-300	-2.4	7.3E-04	-4.1	2.8E-114	-2.4	7.6E-04
PA4223	***pchH***	-7.3	<1.0E-300	-1.3	6.2E-03	-4.3	1.2E-154	-2.6	2.2E-04
PA4224	***pchG***	-7.3	<1.0E-300	-	-	-4.4	4.5E-233	-1.5	1.7E-03
PA4225	***pchF***	-7.4	<1.0E-300	-1.5	3.2E-03	-4.4	2.7E-279	-2.9	1.4E-04
PA4226	***pchE***	-7.5	<1.0E-300	-2.9	6.3E-05	-4.0	7.1E-192	-2.8	1.7E-04
PA4227	***pchR***	-5.4	<1.0E-300	-	-	0.18	0.2	0.5	7.9E-02
PA4228	***pchD***	-6.1	<1.0E-300	-1.3	1.5E-03	-3.4	<1.0E-300	-1.9	2.4E-04
PA4229	***pchC***	-6.4	3.5E-3086	1.3	3.5E-03	-3.2	1.7E-85	-	-
PA4230	***pchB***	-6.6	<1.0E-300	-5.3	1.1E-04	-3.9	<1.0E-300	-3.0	7.4E-06
PA4231	***pchA***	-6.6	<1.0E-300	-2.0	2.1E-03	-3.8	5.2E-268	-2.8	1.1E-04
PVD pathway									
PA2385	***pvdQ***	-9.4	<1.0E-300	-1.5	9.9E-04	-		-	
PA2386	***pvdA***	-10.2	<1.0E-300	-2.4	1.7E-04	-		-	
PA2389	***pvdR***	-7.6	<1.0E-300	-1.4	2.4E-03	-		-	
PA2390	***pvdT***	-7.6	<1.0E-300	-	-	-		-	
PA2391	***opmQ***	-7.7	<1.0E-300	-2.3	1.0E-03	-		-	
PA2392	***pvdP***	-7.7	<1.0E-300	-3.5	1.2E-05	-		-	
PA2394	***pvdN***	-9.6	<1.0E-300	-2.0	3.3E-04	-		-	
PA2395	***pvdO***	-8.9	<1.0E-300	-2.5	5.5E-05	-		-	
PA2396	***pvdF***	-6.8	<1.0E-300	-3.2	2.7E-05	-		-	
PA2397	***pvdE***	-9.9	<1.0E-300	-2.8	8.4E-04	-		-	
PA2398	***fpvA***	-8.9	<1.0E-300	-2.3	2.0E-04	-		-	
PA2399	***pvdD***	-6.9	<1.0E-300	-0.6	3.8E-02	-		-	
PA2400	***pvdJ***	-6.8	<1.0E-300	-2.2	1.7E-04	-		-	
PA2404	***fpvH***	-5.2	9.5E-287	-	-	-		-	
PA2405	***fpvJ***	-5.2	<1.0E-300	-2.2	1.2E-02	-		-	
PA2406	***fpvK***	-5.5	4.7E-162	-	-	-		-	
PA2407	***fpvC***	-4.9	8.0E-134	-	-	-		-	
PA2408	***fpvD***	-4.9	5.4E-116	-2.1	7.5E-03	-		-	
PA2410	***fpvF***	-4.3	6.9E-162	1.6	2.0E-02	-		-	
PA2413	***pvdH***	-6.7	<1.0E-300	-2.8	7.3E-05	-		-	
PA2424	***pvdL***	-9.3	<1.0E-300	-1.8	1.7E-04	-		-	
PA2426	***pvdS***	-9.9	<1.0E-300	-	-	-		-	

Table 2. Expression values from transcriptomic and proteomic analysis of genes of the PVD and PCH pathways in *P. aeruginosa* PAO1 cells grown in CAA medium with or without 10 µM Fe^{3+} or Co^{2+}. '-' indicates a non-significant difference in expression: -1 < log2 fold change < 1.

Legends of figures

Figure 1: Chemical structure of pyoverdine (PVD) and pyochelin (PCH).

Scheme 1. Organization of PCH pathway genes in the *P. aeruginosa* PAO1 genome. *fptABCX*, *pchEFGHI*, *pchR*, and *pchDCBA* are all genes coding for proteins involved in Fe^{3+} acquisition by PCH. Fur is a transcription regulator. Fur loaded with Fe^{2+} represses the expression of all PCH genes via an interaction with the Fur box. PchR is a transcriptional activator of the AraC family. PchR in complex with PCH-Fe^{3+} activates the transcription of all PCH genes, except *pchR*, by interacting with the PchR box (no PchR box upstream of *pchR*).[21–23]

Figure 2. PVD (A) and PCH (B) production by *P. aeruginosa* PAO1 in the absence and presence of different biological metals. Bacteria were grown 24 h in CAA medium with or without 1, 15, or 150 µM of biological metals (no metal (control): black; $FeCl_3$: red; $CoCl_2$: pink; $NiCl_2$: blue; $CuCl_2$: yellow; $MnCl_2$: purple and $ZnCl_2$: green). The concentration of PVD and PCH (µM/$OD_{600\ nm}$) was monitored after 24 h in culture and calculated as described in Materials and Methods.

Figure 3. A. Analysis of fold-change in transcription for genes of the PVD and PCH pathways. *pvdS* and *pvdJ* genes encode a sigma factor and an enzyme involved in PVD pathway. The oder five gens belong to the PVD pathway: *pchR*, encodes the transcriptional regulator, *pchA* and *pchE* are NRPS involved in PCH biosynthesis and *fptA* and *fptX* the outer and inner membrane transporters of PCH-Fe, respectively. RT-qPCR was performed on *P. aeruginosa* PAO1 grown in CAA medium with or without 5 µM $FeCl_3$, $CoCl_2$, $NiCl_2$ or $ZnCl_2$. The data were normalized relative to the reference gene *uvrD* and are representative of three independent experiments. Results are given as a ratio between the values obtained in the presence of metals over those obtained in the absence. All values fold-change values are given in Table 3SM in Supplemental Materials.

B. PchA-mCherry, PchE-mCHERRY and FptX-mCHERRY expression in *P. aeruginosa* cells grown in CAA medium with or without 5 µM $FeCl_3$, $CoCl_2$, $NiCl_2$ or $ZnCl_2$. *pchA-mcherry*, *pchE-mcherry* and *fptX-mcherry* strains were grown in CAA medium. The metals were added at the beginning of culture and bacterial growth monitored at $OD_{600\ nm}$ and the expression of the fluorescent fusion proteins measured by following the fluorescence at 610 nm (excitation at 570 nm). All kinetics are an average of 5 kinetics.

C. mCHERRY-PchR expression in *P. aeruginosa* cells grown in CAA medium with or without $FeCl_3$, $CoCl_2$ or $NiCl_2$. Since the emission of fluorescence in *mcherry-pchR* strain and the variation of fluorescence observed in the presence of Fe^{3+} are low, different metal concentrations were tested. The metals were added at the beginning of culture and bacterial growth monitored at $OD_{600\ nm}$ and the expression of the fluorescent fusion proteins measured by following the fluorescence at 610 nm (excitation at 570 nm). All kinetics are an average of 5 kinetics

Figure 4. A. Transport of PCH-Fe and PCH-Co in *P. aeruginosa* cells. Δ*pvdF*Δ*pchA* (grey bars) and *ΔpvdFΔpchAΔfptA* (white bars) strains at an $OD_{600\ nm}$ of 1 in CAA medium were incubated with or without 4 µM of preformed PCH-metal complexes. For both panels, bacteria were pelleted after a 30-min incubation, washed, and the amount of metal monitored by ICP-AES. **B. Kinetics of intracellular ^{55}Fe accumulation in *P. aeruginosa* cells in the presence of PCH-metal complexes.** Δ*pvdF*Δ*pchA* cells at an $OD_{600\ nm}$ of 1 were incubated with 0.2 µM PCH-^{55}Fe and without (black dots) or with 1 eq. (0.2 µM) or 10 eq. (2 µM) PCH-metal complexes (PCH-Co in green, PCH-Ni in blue, or PCH-Zn in orange). Aliquots were removed at various times and the radioactivity in the cells monitored.

Figure 5. Total content of biological metals in *P. aeruginosa* PAO1 cells grown in CAA medium with or without 5 µM $CoCl_2$. *P. aeruginosa* PAO1 cells were grown in CAA medium without (grey bars) or with 5 µM $CoCl_2$ (black bars). The data are expressed as moles per volume as described previously.[13] The absence of columns for some metals corresponds to the detection limits for low-abundance

elements under these experimental conditions. For all experiments, bacteria were grown in CAA, harvested at the end of the exponential phase, and prepared for ICP-AES measurements as described in Materials and Methods.

Figure 6. Electrophoretic mobility shifts of specific 41bp DNA fragments (g -65 to -31 *pchD* gene promoter containing a Fur box) incubated with Fur protein in the presence of 10 µM $CoCl_2$ or $Mn(OAc)_2$. See the experimental part for details. It is not possible to run EMSA in presence of Fe^{2+} because of its oxidation, consequently, it is well accepted in the literature to use manganese ions to mimic Fe^{2+} for the DNA binding assay.[52]

Figure 7. Expression of mCherry from the pAYC5 plasmid in the absence or presence of $FeCl_3$, $CoCl_2$, $NiCl_2$, or $ZnCl_2$ under Fur regulation. Δ*pchR* cells were transformed with pAYC5 plasmid carrying the *pchD* promoter sequence with the Fur and PchR boxes. These cells were grown in the presence of increasing concentrations of $FeCl_3$, $CoCl_2$, $NiCl_2$ or $ZnCl_2$ (see legend on figure). Bacterial growth was followed at $OD_{600\ nm}$ and mCherry expression by monitoring the emission of fluorescence at 610 nm (excitation at 570 nm).

Figure 8. Expression of mCherry from pAYC5-FURmut plasmid in the absence or presence of $FeCl_3$, $CoCl_2$, $NiCl_2$ or $ZnCl_2$ under PchR regulation. PAO1 (all kinetics with the symbol ● in panels A, B, C and D) and Δ*pchR* (kinetics in grey with the symbol ▲ in panels A, B, C and D) cells were transformed with pAYC5-FURmut plasmid carrying the *pchD* promoter sequence with the PchR box and a Fur mutated box. These cells were grown in CAA medium in the presence of increasing concentrations of $FeCl_3$, $CoCl_2$, $NiCl_2$ or $ZnCl_2$. Bacterial growth was followed at $OD_{600\ nm}$ and mCherry expression by monitoring the emission of fluorescence at 610 nm (excitation at 570 nm). All kinetics are an average of 5 kinetics. No significant variation of mCherry expression was observed in Δ*pchR* mutant in the presence of metals as shown in Supplemental Materials, Figure 4SM.

Scheme 2. The PCH pathway and its interaction with Fe^{3+} and Co^{2+}. PCH can chelate both Fe^{3+} and Co^{2+}. FptA at the bacterial cell surface can interact with both PCH-metal complexes, but with the highest affinity for PCH-Fe, and both complexes are transported efficiently into *P. aeruginosa* cells. The biological function of Fur is not affected by the presence of contaminant Co^{2+} in the bacterial growth medium. PchR can bind PCH-Fe and PCH-Co as well as PCH-Ni, and PCH-Zn, but only PchR-PCH-Fe activates the transcription of PCH genes. The presence of contaminant Co^{2+} in the bacteria growth media leads to the formation of PchR-PCH-Co complexes. This will decrease the intracellular concentration of PchR-PCH-Fe, leading to a decrease in the expression of PCH genes and PCH production.

Significance to Metallomics statement

It is well known that bacteria produce siderophores to get access to iron. Several studies have also shown that the presence of metals other than iron in the bacterial environment can modulate the production of siderophores, but nothing is known concerning the molecular mechanisms involved. We present here how Co^{2+} and Ni^{2+} affects the production of the siderophore pyochelin in *P. aeruginosa* and how these metals interfere specifically or not with different proteins of the pyochelin-dependent iron uptake pathway, including the corresponding transcriptional regulators. We show for the first time, how an excess of biological metals, other than iron, can interfere with transcriptional regulators that control the transcription of genes of a siderophore pathway.

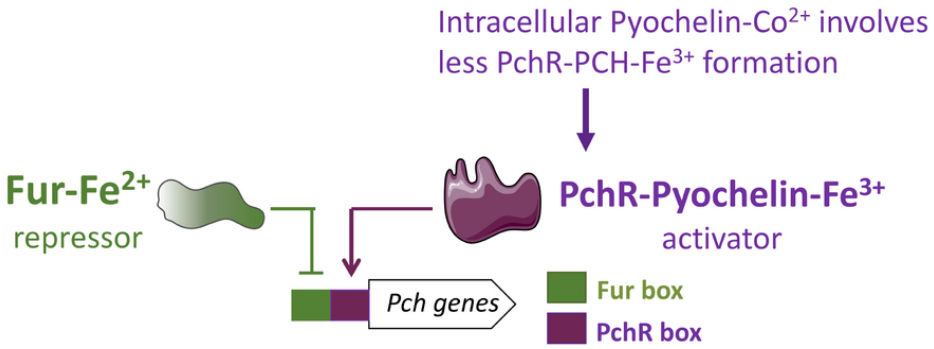

79x32mm (300 x 300 DPI)

Presence of Co^{2+} affects the production of the siderophore Pyochelin in *Pseudomonas aeruginosa*. This repression is not Fur-dependent but due to competition of Pyochelin-Co^{2+} with Pyochein-Fe^{3+} for PchR (transcriptional activator).

Non-specific interference of cobalt with siderophore-dependent iron uptake pathways

Ana Carballido Lopez[a,b], Olivier Cunrath[a,b], Anne Foster[a,b], Julien Pérard[c], Gwenaëlle Graulier[a,b], Rachel Legendre[d,e], Hugo Varet[d,e], Odile Sismeiro[d,e], Quentin Perraud[a,b], Bénédicte Pesset[a,b], Pamela Saint Auguste[f], Dirk Bumann[f], Gaëtan L. A. Mislin[a,b], Jean Yves Coppee[d,e], Isabelle Michaud-Soret[c], Pierre Fechter*[a,b], and Isabelle J.Schalk*[a,b]

[a]Université de Strasbourg, UMR7242, ESBS, Bld Sébastien Brant, F-67413 Illkirch, Strasbourg, France.

[b]CNRS, UMR7242, ESBS, Bld Sébastien Brant, F-67413 Illkirch, Strasbourg, France.

[c]Univ-Grenoble alpes, CNRS, CEA, BIG, CBM, CEA-Grenoble, 38000 Grenoble, France.

[d]Transcriptome and EpiGenome, Biomics, Institut Pasteur, 28 rue du Docteur Roux, 75015 Paris, France.

[e]Institut Pasteur – Bioinformatics and Biostatistics Hub – C3BI, USR 3756 IP CNRS – Paris, France.

[f]Focal Area Infection Biology, Biozentrum, University of Basel, Basel, Switzerland

To whom correspondence should be addressed: Isabelle J. Schalk, UMR 7242, IREBS, ESBS, Blvd Sébastien Brant, CS 10413, F-67412 Illkirch, Strasbourg, France. Tel: 33 3 68 85 47 19; Fax: 33 3 68 85 48 29; E-mail: isabelle.schalk@unistra.fr or p.fechter@unistra.fr

Abstract

Much data shows that biological metals other than Fe^{3+} can interfere with Fe^{3+} acquisition by siderophores in bacteria. Siderophores are small Fe^{3+} chelators produced by the microorganism to obtain access to Fe^{3+}. Here, we show that Co^{2+} is imported into *Pseudomonas aeruginosa* cells in a complex with the siderophore pyochelin (PCH) by the ferri-PCH outer membrane transporter FptA. Moreover, the presence of Co^{2+} in the bacterial environment strongly affects the production of PCH. Proteomic and transcriptomic approaches showed that a decrease of PCH production is associated with repression of the expression of the genes involved in PCH biosynthesis. We used various molecular biology approaches to show that this repression is not Fur- (Ferric uptake transcriptional regulator) dependent but due to competition of PCH-Co with PCH-Fe for PchR (transcriptional activator), thus inhibiting the formation of PchR-PCH-Fe and consequently the expression of the PCH genes. We observed a similar mechanism of repression of PCH production, but to a lesser extent, by Ni^{2+}, but not for Zn^{2+}, Cu^{2+}, or Mn^{2+}. Here, we show, for the first time at a molecular level, how the presence of a contaminant metal can interfere with Fe^{3+} acquisition by the siderophores PCH and PVD.

Introduction

In living organisms, interactions between biomolecules and biological metals (Na, Mg, K, Ca, Mn, Fe, Zn, Ni, Cu, Co, and Mo) are vital and play a role in macromolecule structure and cell metabolism. For example, one third of proteins require metals for their effective functioning. The interactions between macromolecules and metals are highly specific. Waldron and Robinson proposed that to ensure that each metalloprotein or metalloenzyme in bacteria binds the correct metal and functions properly, 'metals are not in competition for a limited pool of proteins, but rather the proteins compete for a limited pool of metals in the cells'.[2,3] Therefore, any disequilibrium of this limited intracellular pool of metals (the bacterial metallome) affects bacterial cell viability. However, bacteria are often subject to variations in metal concentrations in their environment, including during infections, in which they may be confronted with "nutriment immunity", whereby the host uses deprivation of, or poisoning with, metals as defense strategies against microbial invaders.[4,5] For example phagocytes use Cu and/or Zn intoxication to reduce the intracellular survival of pathogens.[6] How bacteria cope with such metal concentration disequilibria at the molecular level and the cross-talk to maintain homeostasis of different biological metals in bacterial cells are still poorly understood.

Bacterial iron homeostasis has attracted the most attention over the last decades. Iron is a key nutriment for bacterial growth, which is paradoxically poorly bioavailable because of its very low solubility under aerobic conditions and physiological pH. Thus, to gain access to Fe^{3+}, most bacteria produce siderophores.[7] These compounds have various chemical structures, a molecular weight usually between 200 and 2 000 Da, and are characterized by an extremely high affinity for Fe^{3+}, with, for example, K_a values of 10^{43} for the siderophores enterobactin.[8] Siderophores provide bacteria with Fe^{3+} by scavenging this metal from the bacterial environment and transporting it into either the bacterial periplasm or cytoplasm.[9,10] This strategy works in any bacterial environment, such as in the rhyzosphere[11], but also plays a key role in the host during infections.[12] *P. aeruginosa*, an opportunistic pathogen and used as a model in the present study, produces two major siderophores, pyoverdine

(PVD) and pyochelin (PCH) (Figure 1).[9] The synthesis of these chelators is correlated with the concentration of iron, both in bacterial cells and the environment.[13] In media with moderately low concentrations of iron (approximately 300 nM), *P. aeruginosa* cells produce more PCH than PVD, whereas in more severely iron-restricted media (approximately 20 nM), PCH production remains highly active and, in addition, PVD production is strongly stimulated.[13,14]

Fe^{3+} uptake into bacteria *via* siderophores always involves a siderophore-specific TonB-dependent transporter for its uptake across the outer membrane in Gram-negative bacteria.[15] Depending on the siderophore, Fe^{3+} is then either delivered into the bacterial periplasm or cytoplasm. Transport into the cytoplasm involves further transport of the ferri-siderophore complex across the inner membrane *via* proton motive force-dependent permeases or ABC transporters.[16] Iron release from siderophores in the bacterial periplasm or cytoplasm requires Fe^{3+} reduction (siderophores having a lower affinity for Fe^{3+} compared to Fe^{2+}), often associated with chemical modification or hydrolysis of the siderophores.[16]

Siderophore production is generally negatively regulated by the presence of Fe^{2+} *via* the Fur transcriptional regulator[19] and positively by iron restriction and the response of various regulatory systems, such as sigma and anti-sigma factors[20], the AraC regulators, or two component systems.[21] Under iron starvation, PCH production is activated via the action of the AraC regulator PchR and PVD by anti-sigma (FpvR) and sigma factors (PvdS and FpvI).[21–23]

An increasing number of studies have also reported that siderophores are able to chelate efficiency metals other than Fe^{3+}.[18] Previously, using the spectral properties of PVD and PCH, we have shown that both PVD and PCH are able to chelate the biological metals Co^{2+}, Cu^{2+}, Ni^{2+} and Zn^{2+} as well as metals like Ag^{+}, Pb^{2+}, Al^{3+}.[24,25] PVD chelates metals with a 1 : 1 stoechiometry and stability constants have been determined for some PVD-metal complexes: PVD-Fe (Ka = $10^{30.8}$ M^{-1}), PVD–Ni^{2+} (Ka = $10^{10.9}$ M^{-1}), PVD–Cd^{2+} (Ka = $10^{8.2}$ M^{-1}), PVD-Cu^{2+} (Ka = $10^{20.1}$ M^{-1}).[26,27] PCH forms predominantly 1 : 2 (M^{2+} /PCH) complexes and the stability constant determined are: for Fe^{3+} (Ka = $10^{28.8}$ M^{-2}), for Zn^{2+} (Ka =

$10^{26.0}$ M^{-2}) and for Cu^{2+} (Ka = $10^{25.0}$ M^{-2}).[28] Baysse *et al.* have shown that PCH can also bind the transition metal vanadium generating a Fenton reaction in the cells.[29] Moreover several studies have shown that the presence of metals other than Fe^{3+} in the bacterial environment can modulate the bacterial production of siderophores, but nothing is known concerning the molecular mechanisms involved.[30–32] For example, PCH synthesis in *P. aeruginosa*, is repressed by 10 μM Fe^{2+}, Co^{2+}, Mo^{+6}, Ni^{2+}, and Cu^{2+}.[33,34] At last, an increasing number of studies have reported that siderophores, in addition to their important role in Fe^{3+} acquisition, also protect bacterial cells against excess toxic metals present in their environment and can consequently play a role in bacterial metal resistance.[13,17,18] Previous studies by our group have shown that both PVD and PCH protect *P. aeruginosa* from toxic metals or an excess of essential metals, to a similar extent, by preventing their intracellular accumulation, thus maintaining the homeostasis of the various biological metals present in bacterial cells.[13,17]

To better understand the possible role of PVD and PCH in the homeostasis of biological metals other than iron, we explored the effect of the presence of various biological metals (Co^{2+}, Cu^{2+}, Ni^{2+}, Mn^{2+} and Zn^{2+}) in bacterial growth media on PVD and PCH production and investigated the possible molecular mechanisms involved in the phenotype(s) observed. Heavy metals were not included in our study, the possible role of the two siderophores in heavy metal resistance being not the focus of this work. We observed that Co^{2+} repressed PCH synthesis with the same efficiency as Fe^{3+}, and repression was also observed with Ni^{2+}, but with lower efficiency. There was no repression by Zn^{2+}, Mn^{2+}, or Cu^{2+}. The repression observed is Fur-independent and due to the ability of Co^{2+} and Ni^{2+} to interfere with the transcriptional regulator PchR (activator of PCH production, Scheme 1). Co^{2+} and Ni^{2+} inhibit PchR-PCH-Fe formation and consequently the concentration of this complex in bacterial cells decreases, resulting in a decrease of the transcription of the genes encoding the enzymes involved in PCH synthesis.

Materials and methods

Chemicals. The metals used were in the following forms: $CoCl_2$,$6H_2O$ (Strem Chemicals), $CuCl_2$,$2H_2O$ (Strem Chemicals), $NiCl_2$,$6H_2O$ (Strem Chemicals), $FeCl_3$ (Alfa Aesar), $Mn(OAc)_2$,$4H_2O$ (Strem Chemicals) and $ZnCl_2$ (Strem Chemicals). All solutions were prepared at concentrations between 1 nM and 100 µM in 0.5 N HCl or 0.5 N HNO_3. These stock solutions were then diluted with 50 mM Tris-HCl pH 8.0. The PCH used in these experiments was synthesized according to a previously published protocol.[35]

Bacterial strains and growth media. *P. aeruginosa* strains used throughout this study are shown in Table 1. For cultures of *P. aeruginosa* strains in iron-limited media, bacteria were first grown in LB broth overnight at 30°C. The bacteria were then washed in CAA medium (casamino acid medium, composition: 5 $g.L^{-1}$ low-iron CAA (Difco), 1.46 $g.L^{-1}$ K_2HPO_4 $3H_2O$, 0.25 $g.L^{-1}$ $MgSO_4$ $7H_2O$), diluted two-fold and incubated for 24 h at 30°C.

Siderophore quantification. The production of PCH and PVD were evaluated as described previously.[25-36] PVD production was monitored by its characteristic absorbance of 400 nm at neutral pH.[36] PCH has a characteristic absorbance of 320 nm, but unlike PVD, this siderophore cannot be detected directly in the bacterial growth medium and needs first to be extracted from the cultures and concentrated before absorbance monitoring.[13,36]

UV and fluorescence spectra of PCH-metal complexes. PCH was solubilized in methanol and PCH-metal complexes were prepared in methanol by mixing 1 eq. of metal with 2 eq. of PCH. 50 mM TrisHCl pH 8.0 buffer was added to reach a concentration of PCH-metal complexes of 50 µM. UV spectra were measured on a Nanodrop 2000 spectrophotometer and fluorescence spectra were measured on a TECAN M200 multiplate reader. All measures were carried out in 50 mM TrisHCl buffer. For emission spectra : λ_{exc} = 350 nm; for excitation spectra : λ_{em} = 422 nm.

Bacterial growth and quantification of fluorescence intensity. Cells were cultured overnight in CAA medium, pelleted by centrifugation, resuspended in fresh CAA medium, and the resulting suspension diluted so as to obtain an optical density at 600 nm of 0.01 units. We dispensed 200 µL of the suspension per well into a 96-well plate (Greiner, U-bottomed microplate) with or without the different metals tested. The plates were incubated at 30°C, with shaking, in a Tecan microplate reader (Infinite M200, Tecan) for measurements of OD_{600nm} and mCherry (excitation/emission wavelengths: 570 nm/610 nm) fluorescence at 30-min intervals, for 40 h. We calculated the mean of three replicates for each measurement.

***Proteomics analysis*.** Bacteria were grown in CAA medium as described above (for growth curve see Figure 1SM in Supplementary Materials). After the first overnight culture in CAA medium, the bacteria were diluted in 10 mL CAA to an $OD_{600\ nm}$ of 0.1 and incubated with or without 10 µM Fe^{3+} or Co^{2+} for 8 h at 30°C. For the digestion and cleanup steps, the same strategy was used as previously described.[37] For the shotgun proteomics assays, 1 µg of peptides of each sample were subjected to LC–MS (liquid chromatography-mass spectrometry) analysis using the same approach as previously described.[37]

Transcriptomic analysis. Bacteria were grown in CAA medium exactly as described above for the proteomic analyses and harvested after 8 h of cultures at 30°C. The total RNA were extracted by hot phenol treatment. Briefly, an aliquot of 8 x 10^8 cells from the cultures were added to two volumes of RNAprotect Bacteria Reagent (Qiagen). After centrifugation, the cell pellets were dissolved in 1 ml of lysis buffer (300 mM NaCl ; 1% SDS ; 8 mM EDTA), incubated at 90°C for 1 min before the addition of 1 mL of phenol and a further incubation at 65°C for 10 min. The extracted RNAs (aqueous phase) were purified again with 1 volume of Phenol/Chloroform. To eliminate any DNA traces, the RNAs were submitted twice to DNaseI treatment. The RNAs were then submitted to ribosomal depletion using the RiboZero Bacteria kit (Illumina). The efficiency of depletion was validated on a Bioanalyzer nanochip (Agilent). Directional cDNA libraries for sequencing were constructed using the TruSeq

Stranded RNA LT Sample Prep kit (Illumina) from enriched non-rRNA samples, following the manufacturer's instructions. After validation of the libraries on a Bioanalyzer DNA1000 chip (Agilent) and QuBit (Invitrogen) quantification, sequencing was performed on a HiSeq 2500 (Illumina). Reads were 65 bp-long in single mode.

Count data were analyzed using R version 3.3.1[38] and the Bioconductor package DESeq2 version 1.12.4.[39] Normalization and the estimation of dispersion were performed with DESeq2, using the default parameters, and statistical tests for differential expression were performed, applying the independent filtering algorithm. A generalized linear model was used to test for the differential expression between the three biological conditions: PAO1 without metals, PAO1 in the presence of Co^{2+} or Fe^{3+}. For each pairwise comparison, raw p-values were adjusted for multiple testing according to the Benjamini and Hochberg (BH) procedure[40] and genes with an adjusted p-value lower than 0.05 were considered to be differentially expressed.

Reads were cleaned of adapter sequences and low-quality sequences using an in-house program (https://github.com/baj12/clean_ngs). Only sequences at least 25 nt in length were considered for further analysis. Bowtie version 0.12.7[41], with default parameters, was used for alignment on the reference genome (*Pseudomonas aeruginosa* PAO1 from NCBI). Genes were counted using featureCounts version 1.4.6-p3[42] from Subreads package (parameters: -t gene -s 1).

Metal quantification by ICP-AES. PCH-metal complexes were prepared by incubating PCH solubilized in methanol with $FeCl_3$, $CoCl_2$, $NiCl_2$ or $ZnCl_2$ at a molar ratio of 2:1 for 15 min. Tris-HCl (50 mM) pH 8.0 buffer was added to bring the siderophore-metal complexes to a final concentration of 4 mM. Δ*pvdF*Δ*pchA* and Δ*pvdF*Δ*pchA*Δ*fptX* cells were grown overnight in CAA media as described above. Cells were then washed and resuspended in CAA medium at an $OD_{600\ nm}$ of 1.5. PCH-Fe or PCH-Co were added to a final concentration of 4 µM and the solutions incubated for 30 min at 30°C with shaking. The samples were then centrifuged and the bacterial pellets washed once with ultrapure water and dried at 50°C for 48 h. Cells were mineralized by incubation in 70% (v/v) HNO_3 for 48 h at room

temperature. The volume was brought up to 10 mL with ultrapure water and the samples filtered through a membrane with a 0.22 µm syringe filter unit. The samples were then analyzed with an ICP-AES apparatus (Varian 720 ES) at the following wavelengths (nm): Co (228.62), Fe (238.20), Ca (393.37), Cd (214.44), Co (228.62), Cr (267.72), Cu (327.40), Fe 238.20), K 766.49), Mg (279.55), Mn (257,61), Mo (202.03), Na (589.59), Ni (231.60), Pb 220.35), V (292.40), and Zn (213.86).

For the data in Figure 4, bacteria were grown in CAA medium in the presence of 5 µM $CoCl_2$. At the end of the exponential phase, samples were centrifuged, and the bacterial pellets treated as described above for the experiment with PCH-Co or PCH-Ni complexes.

$^{55}Fe^{3+}$ uptake. $^{55}FeCl_3$ was obtained from Perkin Elmer Life and Analytical Sciences (Billerica, MA, USA), in solution, at a concentration of 71.1 mM, with a specific activity of 10.18 Ci/g. Siderophore-^{55}Fe complexes were prepared at ^{55}Fe concentrations of 20 µM, with a siderophore: $^{55}Fe^{3+}$ (mol:mol) ratio of 20:1. **$^{55}Fe^{3+}$** uptake assays were carried out as previously described,[43] except that, after growth, bacteria were incubated with 0.2 µM PCH-^{55}Fe and with or without 0.2 and 2 µM PCH-Co or PCH-Zn complexes.

Electrophoresis mobility shift assays (EMSA). EMSA experiments were performed as previously described[44] using a DNA fragment gcgCGCCCGCCAATGATAATAAATCTCATTTCCCAACAgcg containing the -65 to -31 *pchD* promoter region containing a Fur box (underlined) with gcg on both side added for stabilization. DNA radiolabelling was performed by incubating 20-30 nM DNA for 30 min at 37°C in the presence of 1 unit T4 polynucleotide kinase (NEB) and 0.5 µL gamma ATP at 1 mCi /mmol. Labelled DNA was diluted 10 times in binding buffer (20 mM BisTrisPropane pH 8.5, 100 mM KCl, 3 mM $MgCl_2$, 10 µM $CoCl_2$, 5% v/v glycerol, and 0.01% Triton X-100), desalted on G25 mini-spin columns and stored at -20°C. EMSA were performed with 200-250 pM of freshly prepared radiolabelled DNA incubated 30 min at 25°C with various concentrations of Fur protein in binding buffer in the presence of 10 µM Co^{2+} or Mn^{2+}. Fur protein was purified as previously described.[44] After a 30-min incubation at room

temperature, 10 µL of each sample were loaded on an 8 % polyacrylamide (29/1) gel in TA buffer (40 mM Tris acetate pH 8.2) with 10 % glycerol, supplemented with 100 µM of $CoCl_2$. The gel was pre-run 30 min at 100 V in TA buffer supplemented with 100 µM of $CoCl_2$. Mobility shifts were revealed by exposing the gels (2 to 12 h at room remperature) on a storage phosphor screen (GE healthcare) and quantified with a cyclone phosphoimager (Perkin Elmer).

Transcriptional reporters. For the construction of transcriptional reporter plasmid pAYC5 (carrying both PchR and Fur boxes of *pchD* promoter), the promoters of the gene of interest were amplified from the chromosomal DNA of *P. aeruginosa* PAO1 by PCR with specific primers (Table SM2 in Supplemental Materials), allowing overlapping with a second PCR fragment encompassing the open reading frame of mCherry. A second PCR was performed using the two first PCR fragment as template to obtain the transcriptional reporter fragment. This fragment was trimmed by digestion with *Eco*RI and *Hind*III or *Bam*HI and inserted between the sites for these enzymes in pSEVA631 vector to generate pAYC5 and bacteria were transformed with this vector. The mutation of the Fur box of the *pch*D promoters to generate pAYC5-FURmut vector has been obtained with the Q5-site directed mutagenesis kit from New England Biolabs, using specific primers (Table 2SM).

Binding assays with MBP-PchR. The *E. coli* DH5α-pME7180 strain (Table 1), expressing the recombinant protein PchR tagged with MBP at the N-terminal domain,[45] was used to express MBP-PchR protein for the binding assays. The protein was purified (Figure SM3) as described previously[45] and the protocol from Lin *et al.*[46] was used to investigate the binding between MBP-PchR and the different PCH-metal complexes, metals, and apo-PCH. The PCH-metal complexes were generated by mixing 20 mM PCH with $FeCl_3$, $CoCl_2$, $NiCl_2$, or $ZnCl_2$ in methanol at a molar ratio of 2:1 (PCH:metal) to obtain a final metal concentration of 500 µM. The complexes were incubated for 15 min at RT and finally 50 mM Tris-HCl pH 8 was added to adjust the volume to the desired concentration. The complexes were prepared just before use for the binding experiments.

Quantitative real-time PCR. Specific gene expression was measured by RT-qPCR, as previously described.[47] Briefly, overnight cultures of strains grown in CAA medium were pelleted, re-suspended and diluted in fresh medium to obtain an OD_{600nm} of 0.1 units. The cells were then incubated in the presence or absence of 5 µM Fe^{3+} or Co^{2+}, with vigorous shaking, at 30°C for 8 h. RNAs were purified as described previously.[37] We then reverse transcribed 1 µg of total RNA with a High-Capacity RNAto-cDNA Kit, in accordance with the manufacturer's instructions (Applied Biosystems). The amounts of specific complementary DNAs were assessed in a StepOne Plus instrument (Applied Biosystems) with Power Sybr Green PCR Master Mix (Applied Biosystems) and the appropriate primers (Table SM2). The transcript levels for a given gene in a given strain were normalized with respect to those for *uvr*D and are expressed as a ratio (fold change) relative to the reference conditions.

Results

Co^{2+} can repress PCH and PVD production. We first investigated the impact of the biological metals (Co^{2+}, Cu^{2+}, Ni^{2+}, Mn^{2+} and Zn^{2+}) on the production of both siderophores PVD and PCH in iron restricted growth conditions. Bacteria were grown in casamino acids (CAA) medium in the presence of three metal concentrations (Figure 2). CAA contains approximately 20 nM Fe (LB Broth medium contains 4.3 µM)[13] and is considered to be highly iron-restricted. As previously described by Cunrath *et al.,*[13] PAO1 cells produced twice as much PVD as PCH under such growth conditions and in the absence of any biological metal: 116.5 ± 30.7 µM/$OD_{600\ nm}$ and 51.7 ± 3.1 µM/$OD_{600\ nm}$ for PVD and PCH, respectively.

The presence of Fe^{3+} completely repressed PVD production at 1 µM and PCH production only at 15 µM (Figure 2). Co^{2+} was the only other metal able to repress the production of both siderophores, with 41.1%, 48.5%, and 61.4% repression of PVD production in the presence of 1.5, 15, and 150 µM Co^{2+}, respectively. Surprisingly, we observed similar dose-dependent repression for both Fe^{3+} and Co^{2+} for PCH production. Ni^{2+} had no effect on PVD production and only affected PCH biosynthesis at 150 µM, repressing production by 42 %. Mn^{2+} and Zn^{2+} had no significant effect on either PVD or PCH production at the concentrations tested.

Overall, PVD production was repressed, as expected, by the presence of Fe^{3+}, but also to a lesser extent by Co^{2+}, whereas surprisingly PCH production was repressed with equivalent efficiency by Fe^{3+} and Co^{2+} and, to a lesser extent, by the presence of Ni^{2+}.

Genes up- and downregulated in P. aeruginosa cells in the presence of Co^{2+}. We further investigated the impact of the presence of Co^{2+} on *P. aeruginosa* by carrying out proteomic and transcriptomic analyses of bacteria grown in CAA medium with or without 10 µM Fe^{3+} or Co^{2+}. Changes in gene transcription and expression are given as the log2 ratio between *P. aeruginosa* grown with or without Co^{2+} (Table 2). The transcription and expression of several proteins of the PCH pathway was repressed in the presence of Fe^{3+} and Co^{2+}, showing a similar repressive effect of both metals, consistent with

the observed decrease of PCH production (Figure 2). In contrast, the transcription and expression of all genes detected belonging to the PVD pathway were repressed in the presence of Fe^{3+}, as expected, but at a clearly lower level in the presence of Co^{2+}. These data were confirmed by RT-qPCR experiments using several genes: two genes of the PVD pathway (an enzyme involved in PVD biosynthesis *pvdJ* and the transcriptional regulator *pvdS*) and five genes of the PCH pathway (the transcriptional regulator *pchR*, the inner membrane permease *fptX*, the outer membrane transporter *fptA* and two enzymes involved in PCH biosynthesis *pchA* and *pchE*) and the housekeeping gene *uvrD,* which was used for normalization (Figure 3A). RT-qPCR demonstrated a large decrease in transcript levels for all genes of the PCH pathway in the presence of both Fe^{3+} and Co^{2+}, except for the gene encoding the transcriptional regulator *pchR*. Concerning the genes of the PVD pathway, a strong repression is observed for the two genes tested with Fe^{3+} and at a lower extend with Co^{2+}. For Ni^{2+} and Zn^{2+} no significant transcriptional repression of the seven genes tested was observed (Figure 3A), but in some case a very small increase of transcription.

In conclusion, the transcription and expression of the proteins of the PCH pathway (exception for PchR) are more strongly repressed in the presence of Co^{2+}, than the genes of the PVD pathway.

Co^{2+} differently affects the expression of the genes the PCH operons. The RT-qPCR experiment (Figure 3A) highlighted for all genes of the PCH pathway, except for the one corresponding to the transcriptional regulator *pchR*, a large decrease in transcript levels in the presence of Co^{2+} compared to growth conditions in the absence of metals, while the presence of Fe^{3+} repressed the transcription of all genes including *pchR*. This observation indicates that Co^{2+}, and not Fe^{3+}, affects differently the transcription of the genes of PCH operons. The genes of these four PCH genes belong to three different operons: *pchA* and *pchE* belong to the two operons coding for the enzymes involved in PCH biosynthesis *pchDCBA* and *pchEFGHI*, *fptX* to the PCH-Fe *fptABCX* operon, and *pchR* which is not in an operon with other genes (Scheme 1). Co^{2+} is apparently able to repress *fptABCX*, *pchDCBA* and *pchEFGHI* operons and not *pchR.*

To investigate further this observation, we followed the expression of the four proteins PchA, PchE, FptX and PchR of the PCH pathway during bacterial growth, in the presence of the biological metals, using four strains that express fluorescent fusion proteins between mCherry and PchA (*pchA-mCherry* strain*,* Table 1), PchE (*pchE-mcherry*), FptX (*fptX-mCherry*), and the transcriptional regulator PchR (*mCherry-pchR*).[48] These proteins were tagged with mCherry at the N- or C-terminal end, and the tagged proteins chromosomally integrated. The presence of the tag has been shown to affect neither the transcription of the proteins (by RT-qPCR) nor their biological activities (siderophore production or ferri-siderophore uptake).[48] During bacterial growth, in the absence of any metals, two different variation of mCHERRY fluorescence were observed depending on the strains. For *pchA-mCherry, pchE-mcherry* and *fptX-mCherry* strains a strong increase of fluorescence is observed corresponding to an increase of PchA-mCHERRY, PchE-mCHERRY and FptX-mCHERRY fusion protein expression (Figure 3B). On the opposite, for *mcherry-pchR* in the same growth conditions, mCHERRY fluorescence decreased slightly after 6 hours culture (Figure 3C). As expected, the presence of 5 µM Fe^{3+} repressed strongly PchA-mCHERRY, PchE-mCHERRY, mCHERRY-FptX and mCHERRY-PchR fusion protein expression during bacterial growth. Consistent with the RT-qPCR data (Figure 3A), Co^{2+} repressed the expression of PchA-mCHERRY, PchE-mCHERRY and mCHERRY-FptX but not of mCHERRY-PchR. Ni^{2+} and Zn^{2+} at the concentrations tested had no effect on the expression of the four fusion proteins. Actually their presence slightly induced the expression of PchA-mCHERRY, PchE-mCHERRY and mCHERRY-FptX, probably because of the metal-restriction growth conditions.

Based on the *P. aeruginosa* genome, *pchR* expression is regulated solely by Fur (presence only of a Fur-Box) and *pchDCBA*, *pchEFGHI*, and *fptABCX* operons by both Fur and PchR regulators (the presence of both Fur- and PchR-boxes upstream of these genes) (Scheme 1). Our data show that the presence of Co^{2+} inhibits only the transcription of genes that depend on a PchR box for their expression.

Co^{2+} can enter P. aeruginosa cells by the TonB-dependent transporter FptA. According to current knowledge concerning the interaction of the transcriptional regulators Fur and PchR with Fe (formation of Fur-Fe and PchR-PCH-Fe complexes), the interaction of Co^{2+} with one of these regulators includes the importation of Co^{2+} into the bacteria and, in the case of PchR, the presence of PCH-Co to form a PchR-PCH-Co complex.[46] When Co^{2+}, Ni^{2+} and Zn^{2+} are incubated with PCH in solution, the UV spectral modifications observed compared to the UV spectrum of apo PCH, indicates that PCH is able to chelate these three metals (Figure 2SM). Moreover, previously we have determined a Ka of PCH for Zn^{2+} of Ka = $10^{26.0}$ M^{-2} (Ka = $10^{28.8}$ M^{-2} for Fe^{3+}).[28] Previous studies of our group, in which we used ICP-AES (Inductively Coupled Plasma Atomic Emission Spectroscopy, which allows the detection of metals traces), showed that Co^{2+} and Ni^{2+} can both enter *P. aeruginosa* cells *via* the FptA/PCH pathway when bacteria were grown in succinate-containing medium.[24] Here, we used the same approach to verify that bacteria grown in CAA medium are also able to efficiently import Co^{2+} and Ni^{2+}. CAA is 10 fold more iron-restricted than succinate medium: iron concentration of 300 nM for succinate medium and 20 nM for CAA.[13] We used a PVD and PCH-deficient strain (Δ*pvdF*Δ*pchA*, Table 1) to control the presence of siderophores and their concentrations in the assay. The importance of the PCH pathway in metal uptake was evaluated by using the *fptA* (PCH-Fe outer membrane transporter) mutant strain *ΔpvdFΔpchAΔfptA* (Table 1).

As expected, *fptA* deletion markedly affected Fe accumulation in *P. aeruginosa* cells in the presence of PCH (Figure 4A), as well as that of Co^{2+}, showing that Co^{2+} is imported into *P. aeruginosa* cells by the FptA transporter (Figure 4A). Co^{2+} uptake certainly occurs in a complex with PCH, since this transporter recognizes only PCH-metal complexes and not siderophore-free metals.[49,50] However, the amount of Co^{2+} imported by the FptA/Pch system is lower than the amount of Fe^{3+} acquired. We observed no significant FptA-dependent uptake for Ni^{2+} and Zn^{2+} at the metal concentrations tested here, as previously reported.[24]

We also investigated the ability of PCH-Co complexes to compete with and inhibit PCH-^{55}Fe import in *P. aeruginosa* cells. The PVD and PCH-deficient strain (Δ*pvdF*Δ*pchA*) was incubated with 0.2 µM PCH-

^{55}Fe with or without 0.2 µM and 2 µM (1 and 10-fold excess) PCH-metal complexes and the radioactivity incorporated into the bacteria (during a 30-min incubation) counted. Incubation of the bacteria in the presence of PCH-^{55}Fe alone resulted in the uptake of approximately 90 pmol of ^{55}Fe per cell per 30 min (Figure 4B). We observed 60 % inhibition of this uptake in the presence of 2 µM PCH-Co. We also carried out a competition assay with PCH-Ni and PCH-Zn complexes, but observed no significant inhibition of ^{55}Fe uptake *via* PCH.

These data all suggest that, in the range of metal concentrations tested, Co^{2+} and Ni^{2+} can enter bacteria both by diffusion (Co^{2+} and Ni^{2+} accumulation in the *fptA* mutant, Figure 3A) and also *via* the PCH/FptA uptake system for Co^{2+}. Consequently, PCH-Co complexes, as well as siderophore-free Co^{2+} and Ni^{2+}, are present in *P. aeruginosa* cells.

The presence of Co^{2+} in the bacterial environment does not affect the intracellular iron concentration in P. aeruginosa cells. *P. aeruginosa* PAO1 cells were also grown in the presence of 5 µM Co^{2+} or Ni^{2+} to assess how the intracellular concentrations of all biological metals were affected by the presence of an excess of these two metals (Figure 5). Surprisingly, although Co^{2+} can enter bacteria by diffusion or in competition with Fe^{3+} by the FptA/PCH pathway, the intracellular iron concentration was not affected. This suggests that bacteria can adapt to potential competition between Fe^{3+} and Co^{2+} for the FptA/PCH system during growth and that the intracellular iron content is maintained, even in the presence of 5 µM Co^{2+} contamination.

Excess Co^{2+} in the bacterial environment does not affect Fur regulation. We next elucidated the molecular mechanism involved in the Co-dependent repression of PCH pathway expression by investigating the ability of Fur-Co complexes to interact with the Fur boxes *in vitro*. *E. coli* Fur has been shown to bind DNA sequences containing Fur boxes by interacting with metals other than Fe^{2+} [51] and Fur of *P. aeruginosa* has been shown to be capable of binding to the Fur box in the presence of Co^{2+} in a nuclease protection assay[44] and in the presence of Mn^{2+} in an EMSA (electrophoretic mobility shift

assay) assay.[52] It is not possible to run EMSA in the presence of Fe^{2+} because of its oxidation. Consequently, it is well accepted in the literature to use Mn^{2+} ions to mimic Fe^{2+} for the DNA binding assay.[52] Here EMSA experiments were carried out in the presence of Co^{2+} and Mn^{2+}, with purified Fur protein and the promoter region of *pchD*, containing the Fur-box present upstream of the *pchDCBE* operon. An interaction between Fur-Co and the *pchD* promoter sequence was observed (Figure 6), proving that Fur-Co is able to bind to this sequence. However, our proteomic, transcriptomic and RT-qPCR data (Table 2 and Figure 3A), as well as the expression data using mCherry fusion proteins (Figure 3B-3C), clearly show that the presence of Co^{2+} in the bacterial environment does not repress all Fur-dependent genes, as does the presence of Fe^{3+}. Therefore, we also used a plasmid (pAYC5) carrying the mCherry sequence and the PCH promoter of *pchDCBA* operon (Table 1SM) to investigate the behavior of Fur in the presence of Co^{2+} in *P. aeruginosa* cells. Since this promoter region also contains a PchR box, we carried out this experiments in strain unable to express PchR (Δ*pchR* strain). Bacteria carrying this construct were grown in CAA medium with increasing concentration (0-100 µM) of Co^{2+} or Fe^{3+} and the mCherry fluorescent signal monitored at 610 nm (excitation at 570 nm). As expected, the addition of Fe^{3+} to the bacterial growth medium caused the repression of mCherry expression (Figure 7A): the Fur-Fe complex interacts with the bacterial Fur boxes, which represses the transcription and expression of mCherry and any Fur-dependent genes. The addition of Co^{2+} to the bacterial medium had no significant effect on mCherry expression (Figure 7B) for concentrations of Co^{2+} equivalent or lower than 10 µM and a weak effect was observed at 100 µM. We carried out the same experiment with 10 and 100 µM Ni^{2+} or Zn^{2+} (Figure 7C and 7D) and no repression of mCherry expression was observed.

Overall, our data show that, Fur-Co can bind to the PCH Fur-box but does not repress Fur-dependent gene expression *in vivo* like Fe^{2+} whereas equivalent effects are observed for both metals for PCH production (Figure 2).

The purified cytoplasmic regulator PchR can bind to PCH-Co and PCH-Ni in addition to PCH-Fe. PchR,

the transcriptional activator of the genes of the PCH pathway, activates the transcription of all PCH genes, except *pchR*, by interacting with the PchR box (no PchR box upstream of *pchR* gene).[21–23] We carried out binding assays between purified PchR (MBP fused PchR[46] and purified protein shown in Figure SM3) and PCH-Co and PCH-Ni, based on a spectroscopy approach previously described, using the fluorescent properties of the tryptophans (Trp) of PchR published previously.[46] When MBP-PchR is excited at 280 nm, tryptophan present in the protein emits intrinsic fluorescence with maximal intensity at 330 nm (Figure 4SM). Upon the addition of ligands, such as PCH-Fe, the fluorescence is quenched. Thus, the protein's affinity for its ligand can be determined by plotting the relative fluorescence intensity, F_0/F, with F_0 being the fluorescence emitted by MBP-PchR without ligand and F the fluorescence emitted by MBP-PchR once a specific concentration of ligand has been added. Afterwards, K_d values are determined using the Stern-Volmer representation and linear regression. PCH-metal complexes were prepared by incubating 2 equivalent of PCH with one of metal (Figure 2SM).

We determined an affinity of PCH-Fe (K_d = 5.82 ± 2.84 µM) for MBP-PchR that was slightly better as that described previously (K_d = 41 ± 5 µM)[46]. PCH-Co was also able to bind to PchR with a K_d of 13.9 ± 3.4 µM, as well as PCH-Ni and PCH-Zn (Kd values of 42 ± 4.3 µM and 47.4 ± 2.2 µM, respectively -for details see Figure 4SM). We were unable to investigate the ability of PchR-PCH-Co to bind the PchR box (EMSA assays with the purified MBP fused PchR protein), probably because of the presence of the tag, as well as problems with protein aggregation.

Role of PchR in the repression of the PCH pathway in the presence of Co^{2+} and Ni^{2+}. We further explored the mechanism involved in the repression of PCH production observed in the presence of Co^{2+} and Ni^{2+} by constructing a plasmid (pAYC5-FURmut) carrying the mCherry sequence and the promoter of the *pchDCBA* operon containing only the PchR box and the Fur box having being mutated (Table 1SM and 2SM). The strains PAO1 and Δ*pchR* (unable to express PchR) carrying this plasmid were grown in CAA medium supplemented with increasing concentrations of metals (Fe^{2+}, Co^{2+}, Ni^{2+}

or Zn^{2+}). In the absence of metals, in the WT (PAO1) background (kinetics with black dots in Figure 8A-8D), the fluorescence corresponding to mCherry expression highly increased in function of time, but not in the Δ*pchR* strain unable to express the transcriptional activator PchR (kinetics with grey triangles in Figure 8A-8D), indicating that PchR is necessary to observe mCherry expression. For PAO1, in the presence of increasing concentrations of Fe^{3+}, this fluorescence corresponding to mCherry expression decreased during bacterial growth (Figure 8A). This observation is due to Fur which gets loaded with Fe^{2+}, interacts with its promoter regions and consequently the expression of PchR and the other proteins of the PCH pathway is repressed (Figure 3A and Table 2). Since less PchR is expressed, *mcherry* transcription is no more activated and lower level of fluorescence are observed compared to the condition in the absence of metal.

In the presence of increasing concentrations of Co^{2+} or Ni^{2+} (but not Zn^{2+}; Figure 8B-8D), the fluorescence corresponding to mCherry expression also decreased in PAO1 cultures, but less than in the presence of Fe^{3+}. Higher concentrations of Co^{2+} (10 µM) and Ni^{2+} (100 µM) are necessary to elicit an effect equivalent to that observed with Fe^{3+} (5 µM). In that case, the decrease of fluorescence is not due to an absence of PchR expression, since Co^{2+} or Ni^{2+} present in the *P. aeruginosa* environment were both unable to repress the expression of Fur-regulated genes (Figure 7). Co^{2+} (and probably also Ni^{2+}) are likely present in the bacterial cytoplasm, mostly in their PCH-complexed forms (50 µM is the concentration of PCH in the bacterial culture and 5 µM metals are added to the growth media). Increasing concentrations of PCH-Co or PCH-Ni complexes in the bacterial cytoplasm certainly leads to an increase in the concentrations of PchR-PCH-Co or PchR-PCH-Ni complexes, at the expense of PchR-PCH-Fe complexes, but only PchR-PCH-Fe complexes are probably able to activate transcription of the genes for the proteins of the PCH pathway and *mcherry* from pAYC5-FURmut plasmid. In such a scenario, the expression of PchR-regulated genes, as the genes of the PCH pathway, is less highly activated and less PCH is produced (Figure 2). This also explains why the presence of Co^{2+} or Ni^{2+} does not repress *pchR* expression, as the transcription of this gene is not regulated by the PchR promoter, but only the Fur box (Scheme 1).[45]

In conclusion, the presence of high levels of Fe^{3+}, Co^{2+}, or Ni^{2+} (to a lesser extent) in the bacterial environment induces repression of the transcription of PCH genes (except *pchR*) by two different molecular mechanisms. In the presence of Fe^{3+} in the bacterial environment, the transcriptional repressor Fur, in a complex with Fe^{2+}, represses the expression of these genes. In the presence of Co^{2+} or Ni^{2+}, Fur is not involved, but rather the transcriptional activator PchR, which is no more able to activate the production of PCH, probably due to a decrease in the intracellular concentration of PchR-PCH-Fe complexes.

Discussion

The requirement for different biological metals in bacteria are very different and depend on their biological function. The relative intracellular concentrations of these metals in *P. aeruginosa* PAO1 cells are Na-K > Mg >> Ca >> Fe-Zn >> Mn-Mo-Cu-V-Cr-Ni >> Co[13], with Fe and Zn being the two most abundant transition metals (concentrations between 10^{-3} and 10^{-4} M, depending on the growth medium). The intracellular concentrations of Cu, Mn, Mo, and Ni are generally between 10^{-5} and 10^{-4} M[13] and Co is used only in very small amounts by *P. aeruginosa* (a concentration too low to be detected by ICP-AES[13]). Very similar values have been described for wild type *E. coli*[53] and can probably be found in many Gram-negative bacteria in planktonic growth conditions.

Since, all biological metals become toxic at high concentrations and are highly deleterious to living organisms, the intracellular concentrations of these biological metals have to be finely regulated to stay constant. Siderophores play a key role in iron homeostasis.[21] Increasing number of publications also suggest that siderophores may play a role in the homeostasis of other biological metals.[18] Indeed, these compounds are able to chelate many metals other than Fe^{3+},[18] their production can be modulated by different metals[30–34] and they often play a role in bacterial metal resistance.[17,18] These observations lead to the question whether bacteria are able to activate their siderophore production in response to the presence of metals other than Fe^{3+}. As in previous studies,[24] we showed that none of the metals tested was able to significantly activate PVD or PCH production above that induced by iron restriction (Figure 2). Moreover, there is currently no data available to support the existence of bacterial sensors that detect toxic metals in the bacterial environment and consequently activate siderophore production. All current data suggest that for example the protective role of siderophores against toxic metals is probably only a consequence of the presence of large amounts of siderophores produced in response to iron starvation. However, the formation of siderophore-metal complexes with metals other than Fe^{3+} may increase the sense of iron starvation by bacteria, because siderophores are in complex with metals other than Fe^{3+} and consequently less siderophore-Fe is imported into the bacteria.

In the present work, Co^{2+} and Ni^{2+} were able to repress the production of PCH and for Co^{2+}, with the same efficiency as Fe^{3+}. PCH production is positively regulated by the transcriptional activator PchR and negatively by the transcriptional repressor Fur (Scheme 1). PchR activates the transcription of all PCH genes, except *pchR*, by interacting with the PchR box (no PchR box upstream of *pchR*, Scheme 1). Consequently, a decrease of PCH production must be due to either Fur-dependent repression or the inability of PchR to still activate PCH production. Our data show that Fur regulation is insensitive to the presence of excess Co^{2+} (or Ni^{2+}), even if Co^{2+} bound to Fur proteins *in vitro* and formed complexes with Fur boxes. Our experimental data show that the repression of PCH production by Co^{2+} and Ni^{2+} involves PchR. They also show that PCH-Co enters bacteria via the TonB-dependent outer membrane transporter FptA and can bind to PchR *in vitro*. Since a repression of PCH production is as well observed in the presence of Ni^{2+}, we cannot exclude that PCH-Ni is also able to enter *P. aeruginosa* cells but with uptake rates too low to be detected by our approach. Altogether, these data describe a mechanism in which PCH-Co, after entering *P. aeruginosa* cells by FptA, interacts with PchR to form PchR-PCH-Co complexes unable to activate the transcription of PchR-regulated genes. The formation of PchR-PCH-Co or PchR-PCH-Ni complexes in the bacterial cytoplasm certainly leads to a decrease in the intracellular concentration of PchR-PCH-Fe, leading to a decrease in the transcription of PCH pathway genes and, thus, the production of PCH.

The repression of PCH production was more pronounced with Co^{2+} than Ni^{2+} and cannot be explained simply by the difference in affinities of PchR for the PCH-Co and PCH-Ni complexes. Previous studies, based on titration experiments, have shown that the binding affinity of PCH is higher for Ni^{2+} than Co^{2+} (relative affinity of PCH for biological metals having been proposed Fe(III) > Mo(VI) = Cu(II) > Ni(II) > Co(II) > Zn(II) > Mn(II).[33] On the contrary, the PCH-Co complex more efficiently competes with PCH-Fe for the TonB-dependent transporter FptA (affinities of PCH-Co and PCH-Ni for FptA in the range of 15 nM and 50 nM, respectively[24]) and is more efficiently transported into *P. aeruginosa* cells. The higher efficiency of Co^{2+} to repress PCH production is probably linked to its higher ability to enter *P. aeruginosa* cells as a PCH-Co complex relative to PCH-Ni.

ICP-AES measurements of intracellular metal concentrations of *P. aeruginosa* cells grown with or without Co^{2+} showed no effect of this metal on the intracellular iron concentration. This indicates that the inhibition of PCH production in the presence of Co^{2+} has little effect on bacterial iron homeostasis under our growth conditions. The ability of Co^{2+} to interfere with Fe^{3+} acquisition *via* the PCH/FptA pathway (55 % inhibition of PCH-^{55}Fe uptake in *P. aeruginosa* PAO1 cells when incubated for 30 min in the presence of PCH-Co complexes) does not affect the access to iron of the pathogen. This organism uses several strategies to obtain access to iron; if one iron acquisition pathway is compromised, the bacteria simply uses another.[12]

FptA plays a key role in the outer membrane for the uptake of the right metal by PCH. Previous studies from our group have shown that FptA at the bacterial surface can bind different PCH-metal complexes, with affinities ranging from 10 nM to 4.8 μM, (the affinity of PCH-Fe being 10 nM).[24] However, only Fe^{3+} and, to a lesser extent, Co^{2+} can accumulate significantly in *P. aeruginosa* cells via the PCH pathway, but with uptake rates clearly lower than those for Fe^{3+}. Moreover, previous studies have also shown that PCH complexes Ga^{3+} and the formed complex is transported into *P. aeruginosa* cells via FptA.[24,54] Ni^{2+} is probably also transported in complex with PCH with low uptake rates, since the presence of this metal in the bacterial environment represses PchR regulated genes. FptA, due to its uptake specificity, avoids and controls the uptake of most metals other than Fe^{3+} across the outer membrane and limits the uptake of Co^{2+} and Ni^{2+}. Fe^{3+}, Co^{2+} and Ni^{2+} are part of the iron triad and all three elements show similar properties such as the metallic radius (124, 125, 125 pm, respectively) and the electronic configuration. Ga^{3+} has a radius slightly larger (187 ppm) than Fe^{3+} but very similar coordination properties. Consequently, PCH-Co, PCH-Ni and PCH-Ga have certainly very close conformations, which is not the case for PCH-Cu and PCH-Zn complexes (two metals with different coordination properties compared to Fe^{3+}). The metallic radius and similar coordination properties could be responsible for the high specificity of FptA for PCH-metal complexes.

We are aware that the µM concentrations of Co^{2+} and Ni^{2+} used in this study are not truly physiological in the natural environment thrived by *P. aeruginosa,* and exposure to such concentrations appears unlike during infections and exceptional also in natural environment. However, such concentrations are often used in the literature in studies investigating the role of siderophores in bacterial resistance to metals or in development of bioremediation processes using siderophore producing bacteria to decontaminated metal polluted media or wastes. In such contexts, it is important to understand how siderophore production and siderophore-dependent Fe^{3+} uptake pathways in bacteria interfere with an excess of metals other than Fe^{3+} and what are the molecular mechanisms involved.

Conclusion

We show for the first time, how an excess of biological metals, other than iron, can interfere with transcriptional regulators that control the transcription of genes of the PCH pathway. The presence of high levels of Fe^{3+}, Co^{2+}, or Ni^{2+} (to a lesser extent) in the bacterial environment represses the transcription of PCH genes by two different molecular mechanisms. In the presence of increasing Fe^{3+} concentrations, the transcriptional repressor Fur gets loaded with Fe^{2+} and represses the expression of all *pch* genes. In the presence of increasing Co^{2+} or Ni^{2+} concentrations, Fur is not involved, but the transcriptional activator PchR gets loaded with PCH-Co and PCH-Ni and consequently is no more able to activate the transcription of *pch* genes, due to a decrease in the intracellular concentration of PchR-PCH-Fe complexes.

PchR appears to have broad metal-binding specificity, but since only a few metals (Fe^{3+}, Ga^{3+}, Co^{2+}, and Ni^{2+}) are able to enter bacteria by the FptA/PCH pathway, most which could be present as a contaminant in the bacterial environment do not affect PCH production. Indeed, FptA acts as a selective gate for the uptake of PCH-metal complexes and allows the uptake of only PCH-Fe and, to a lesser extent, PCH-Ga, PCH-Co, and PCH-Ni. The presence of these PCH-metal complexes in the bacterial cytoplasm interferes with the regulation of PCH production by interacting with PchR and inhibiting the positive autoregulatory loop that involves PchR (Scheme 2). The inability of PchR-PCH-

Co and PchR-PCH-Ni to activate the expression of PCH genes highly suggests that PCH is not involved in the acquisition by *P. aeruginosa* of these two metals, but that their uptake via PCH is simply a non-specific interference of these two metals with the PCH pathway. Moreover, the Achilles heel of the *P. aeruginosa* PCH pathway, in terms of excess Co^{2+} in the bacterial environment, is the selectivity of FptA for metal transport. However, the ability of PchR to interact with many different PCH-metal complexes leads to a decrease in PCH production and consequently a decrease in PCH-Co and PCH-Ni import.

Conflicts of interest

There are no conflicts to declare.

Acknowledgments

This work was partly funded by the *Centre National de la Recherche Scientifique*. O. Cunrath held a fellowship from the French *Ministère de la Recherche et de la Technologie* (3 years) and the FRM (*Fondation pour la Recherche Médical*, 6 months). A.Y Carballido Lopez held a fellowship from the University of Strasbourg (IDEX) and B. Pesset from the DGA (Direction Générale des l'Armement). J.P. and I.M.S. thank the Laboratory of Excellence GRAL (grant ANR-11-LABX-49-01) and the Labex ARCANE (grant ANR-11-LABX-0003-01). The Transcriptome and Epigenome Platform is a member of the France Génomique consortium (ANR10-NBS-09-08). We thank Dr A. Boos and P. Ronot (Institut Pluridisciplinaire Hubert Curien, Strasbourg) for their help in the ICP-AES measurements.

Author contributions

ACL evaluated the siderophore production in the presence of metals, performed the iron uptake assays, the experiment with the fluorescent strains (Figure 2) and binding assays with MBP-PchR. OC performed the metal uptake assays and metal quantifications. AF realized the molecular biology

(plasmid and strain constructions) and the fluorescent experiments in Figure 7 with GG. RL, HV, OS, JYC performed the transcriptional experiments and analyses. PMS and DB performed the proteomic experiments and analysis. JP and IM-S performed the electrophoresis mobility shift assays. BP and GLAM synthesized the PCH used in the experiments. QP realized the spectral characterization of PCH-metal complexes. PF realized the RT-qPCR experiment and participated in the design of all experiments and the analysis of all data. IJS directed the project, analyzed data and wrote the paper. All authors discussed the results and contributed to the writing of the manuscript.

References

1 C. L. Dupont, S. Yang, B. Palenik and P. E. Bourne, *Proc. Natl. Acad. Sci. U. S. A.*, 2006, **103**, 17822–17827.
2 N. J. Robinson, *Nat Chem Biol*, 2007, **3**, 692–3.
3 K. J. Waldron, J. C. Rutherford, D. Ford and N. J. Robinson, *Nature*, 2009, **460**, 823–30.
4 E. D. Weinberg, *Biochim. Biophys. Acta*, 2009, **1790**, 600–605.
5 T. E. Kehl-Fie and E. P. Skaar, *Curr. Opin. Chem. Biol.*, 2010, **14**, 218–224.
6 K. Y. Djoko, C. Y. Ong, M. J. Walker and A. G. McEwan, *J. Biol. Chem.*, 2015, **290**, 18954–18961.
7 R. C. Hider and X. Kong, *Nat Prod Rep*, 2011, **27**, 637–57.
8 K. N. Raymond, E. A. Dertz and S. S. Kim, *Proc Natl Acad Sci U A*, 2003, **100**, 3584–8.
9 P. Cornelis, *Appl Microbiol Biotechnol*, 2010, **86**, 1637–45.
10 I. J. Schalk and L. Guillon, *Amino Acids*, 2013, **44**, 1267–1277.
11 P. E. Powell, G. R. Cline, C. P. P. Reid and P. J. Szaniszlo, *Nature*, 1980, **287**, 833–834.
12 P. Cornelis and J. Dingemans, *Front Cell Infect Microbiol*, 2013, **3**, 75.
13 O. Cunrath, V. A. Geoffroy and I. J. Schalk, *Environ. Microbiol.*, 2016, **18**, 3258–3267.
14 Z. Dumas, A. Ross-Gillespie and R. Kümmerli, *Proc. Biol. Sci.*, 2013, **280**, 20131055.
15 I. J. Schalk, G. L. A. Mislin and K. Brillet, *Curr. Top. Membr.*, 2012, **69**, 37–66.
16 I. J. Schalk and L. Guillon, *Environ. Microbiol.*, 2013, **15**, 1661–1673.
17 A. Braud, V. Geoffroy, F. Hoegy, G. L. A. Mislin and I. J. Schalk, *Env. Microbiol Rep.*, 2010, **2**, 419–425.
18 I. J. Schalk, M. Hannauer and A. Braud, *Env. Microbiol*, 2011, **13**, 2844–54.
19 M. F. Fillat, *Arch. Biochem. Biophys.*, 2014, **546**, 41–52.
20 M. A. Llamas, F. Imperi, P. Visca and I. L. Lamont, *FEMS Microbiol Rev*, 2014, **38**, 569–97.
21 P. Cornelis, S. Matthijs and L. Van Oeffelen, *Biometals*, 2009, **22**, 15–22.
22 P. Visca, *Pseudomonas Vol. 2 Ed. Juan-Luis Ramos Kluver Acad. Publ. New-York*, 2004, 69–123.
23 Z. A. Youard and C. Reimmann, *Microbiol. Read. Engl.*, 2010, **156**, 1772–1782.
24 A. Braud, M. Hannauer, G. L. A. Mislin and I. J. Schalk, *J Bacteriol*, 2009, **191**, 5317–25.
25 A. Braud, F. Hoegy, K. Jezequel, T. Lebeau and I. J. Schalk, *Env. Microbiol*, 2009, **11**, 1079–91.
26 A. M. Albrecht-Gary, S. Blanc, N. Rochel, A. Z. Ocacktan and M. A. Abdallah, *Inorg Chem*, 1994, **33**, 6391–6402.

27 C. Ferret, J. Y. Cornu, M. Elhabiri, T. Sterckeman, A. Braud, K. Jezequel, M. Lollier, T. Lebeau, I. J. Schalk and V. A. Geoffroy, *Env. Sci Pollut Res Int*, , DOI:10.1007/s11356-014-3487-2.

28 J. Brandel, N. Humbert, M. Elhabiri, I. J. Schalk, G. L. A. Mislin and A.-M. Albrecht-Garry, *Dalton Trans*, 2012, **41**, 2820–34.

29 C. Baysse, D. De Vos, Y. Naudet, A. Vandermonde, U. Ochsner, J. M. Meyer, H. Budzikiewicz, M. Schafer, R. Fuchs and P. Cornelis, *Microbiology*, 2000, **146 (Pt 10)**, 2425–34.

30 M. Huyer and W. J. Page, *Appl Env. Microbiol*, 1988, **54**, 2625–2631.

31 M. Hofte, S. Buysens, N. Koedam and P. Cornelis, *Biometals*, 1993, **6**, 85–91.

32 X. Hu and G. L. Boyer, *Appl Env. Microbiol*, 1996, **62**, 4044–4048.

33 P. Visca, G. Colotti, L. Serino, D. Verzili, N. Orsi and E. Chiancone, *Appl Env. Microbiol*, 1992, **58**, 2886–93.

34 G. M. Teitzel, A. Geddie, S. K. De Long, M. J. Kirisits, M. Whiteley and M. R. Parsek, *J Bacteriol*, 2006, **188**, 7242–56.

35 A. Zamri and M. A. Abdallah, *Tetrahedron*, 2000, **56**, 249–256.

36 F. Hoegy, G. L. Mislin and I. J. Schalk, *Methods Mol Biol*, 2014, **1149**, 293–301.

37 V. Gasser, E. Baco, O. Cunrath, P. S. August, Q. Perraud, N. Zill, C. Schleberger, A. Schmidt, A. Paulen, D. Bumann, G. L. A. Mislin and I. J. Schalk, *Environ. Microbiol.*, 2016, **18**, 819–832.

38 R Core Team, .

39 M. I. Love, W. Huber and S. Anders, *Genome Biol.*, 2014, **15**, 550.

40 Y. Benjamini and Y. Hochberg, *J. R. Stat. Soc.*, 1995, **57**, 289–300.

41 B. Langmead, C. Trapnell, M. Pop and S. L. Salzberg, *Genome Biol.*, 2009, **10**, R25.

42 Y. Liao, G. K. Smyth and W. Shi, *Bioinforma. Oxf. Engl.*, 2014, **30**, 923–930.

43 F. Hoegy and I. J. Schalk, *Methods Mol Biol*, 2014, **1149**, 337–46.

44 J. Pérard, J. Covès, M. Castellan, C. Solard, M. Savard, R. Miras, S. Galop, L. Signor, S. Crouzy, I. Michaud-Soret and E. de Rosny, *Biochemistry*, 2016, **55**, 1503–1515.

45 L. Michel, N. Gonzalez, S. Jagdeep, T. Nguyen-Ngoc and C. Reimmann, *Mol Microbiol*, 2005, **58**, 495–509.

46 P.-C. Lin, Z. A. Youard and C. Reimmann, *Biometals Int. J. Role Met. Ions Biol. Biochem. Med.*, 2013, **26**, 1067–1073.

47 H. Gross and J. E. Loper, *Nat Prod Rep*, 2009, **26**, 1408–46.

48 O. Cunrath, V. Gasser, F. Hoegy, C. Reimmann, L. Guillon and I. J. Schalk, *Env. Microbiol*, 2015, **17**, 171–85.

49 D. Cobessi, H. Celia, N. Folschweiller, M. Heymann, I. Schalk, M. Abdallah and F. Pattus, *Acta Crystallogr Biol Crystallogr*, 2004, **60**, 1467–9.

50 K. Brillet, C. Reimmann, G. L. A. Mislin, S. Noël, D. Rognan, I. J. Schalk and D. Cobessi, *J Am Chem Soc*, 2011, **133**, 16503–9.

51 A. Adrait, L. Jacquamet, L. Le Pape, A. Gonzalez de Peredo, D. Aberdam, J. L. Hazemann, J. M. Latour and I. Michaud-Soret, *Biochemistry*, 1999, **38**, 6248–6260.

52 U. A. Ochsner, A. I. Vasil and M. L. Vasil, *J Bacteriol*, 1995, **177**, 7194–201.

53 C. E. Outten and T. V. O'Halloran, *Science*, 2001, **292**, 2488–92.

54 E. Frangipani, C. Bonchi, F. Minandri, F. Imperi and P. Visca, *Antimicrob. Agents Chemother.*, 2014, **58**, 5572–5575.

55 C. K. Stover, X. Q. Pham, A. L. Erwin, S. D. Mizoguchi, P. Warrener, M. J. Hickey, F. S. Brinkman, W. O. Hufnagle, D. J. Kowalik, M. Lagrou, R. L. Garber, L. Goltry, E. Tolentino, S. Westbrock-Wadman, Y. Yuan, L. L. Brody, S. N. Coulter, K. R. Folger, A. Kas, K. Larbig, R. Lim, K. Smith, D. Spencer, G. K. Wong, Z. Wu, I. T. Paulsen, J. Reizer, M. H. Saier, R. E. Hancock, S. Lory and M. V. Olson, *Nature*, 2000, **406**, 959–64.

56 V. Gasser, L. Guillon, O. Cunrath and I. J. Schalk, *J Inorg Biochem*, 2015, **148**, 27–34.

57 E. Martínez-García, T. Aparicio, A. Goñi-Moreno, S. Fraile and V. de Lorenzo, *Nucleic Acids Res.*, 2015, **43**, D1183-1189.

58 L. Guillon, S. Altenburger, P. L. Graumann and I. J. Schalk, *PLoS ONE*, 2013, **8**, e79111.

Strains	Coll. Ref.	Description	Ref.
PAO1	PAS43	ATCC15692. *P. aeruginosa* wild-type strain	55
ΔpvdFΔpchAΔfptA	PAS273	Deletion of *pvdF*, *pchA* and *fptA* genes	48
ΔpvdFΔpchA	PAS283	Deletion of *pvdF* and *pchA* genes in PAO1	48
pchA-mCherry	PAS193	Derivate of PAO1 *wt*; *pchAmcherry* chromosomally integrated	56
pchE-mcherry	PAS195	Derivate of PAO1 *wt*; *pchEmcherry* chromosomally integrated	48
fptX-mCherry	PAS210	Derivate of PAO1 *wt*; *fptXmcherry* chromosomally integrated	48
mCherry-pchR	PAS208	Derivate of PAO1 *wt*; *mcherrypchR* chromosomally integrated	48
ΔpchR	PAS387	Deletion of *pchR* in PAO1	48
E. coli DH5α	-	Strain with pME7180 plasmid carrying *MBP* added to the *5'pchR* under the effect of the lac promoter induced by IPTG	45
E. coli HB101		Helper strain carrying pME487	Promega
E.coli Top10	-	F- mcrA Δ(mrr-hsdRMS-mcrBC) ϕ80lacZΔM15 ΔlacX74 nupG recA1 araD139 Δ(ara-leu)7697 galE15 galK16 rpsL(StrR) endA1 λ	Invitrogen
Plasmids			
pAYC5	pAYC5	*pchD* promoter containing the Fur box and PchR box fused to mCherry ORF	This study
pAYC5-FURmut	pAYC5-FURmut	*pchD* promoter containing the Fur mutated box and PchR box fused to mCherry ORF	This study
pSEVA631	244	Low copy plasmid for *E. coli / Pseudomonas spp.*	57
pLG3	154	Expression vector carrying mCherry sequence	58

Table 1. Bacterial strains and plasmids used in this study.

		Down regulated genes							
		PAO1							
		Fe^{3+}				Co^{2+}			
		Transcriptome		Proteome		Transcriptome		Proteome	
ID		log2 fc	p-value	log2 ratio	p-value	log2 fc	p-value	log2 ratio	p-value
PCH pathway									
PA4218	***fptX***	-7.5	<1.0E-300	-2.1	2.2E-02	-3.8	2.3e-297	-1.9	1.7E-02
PA4221	***fptA***	-7.9	<1.0E-300	-2.9	1.5E-04	-4.2	<1.0E-300	-3.2	1.0E-04
PA4222	***pchI***	-7.5	<1.0E-300	-2.4	7.3E-04	-4.1	2.8E-114	-2.4	7.6E-04
PA4223	***pchH***	-7.3	<1.0E-300	-1.3	6.2E-03	-4.3	1.2E-154	-2.6	2.2E-04
PA4224	***pchG***	-7.3	<1.0E-300	-	-	-4.4	4.5E-233	-1.5	1.7E-03
PA4225	***pchF***	-7.4	<1.0E-300	-1.5	3.2E-03	-4.4	2.7E-279	-2.9	1.4E-04
PA4226	***pchE***	-7.5	<1.0E-300	-2.9	6.3E-05	-4.0	7.1E-192	-2.8	1.7E-04
PA4227	***pchR***	-5.4	<1.0E-300	-	-	0.18	0.2	0.5	7.9E-02
PA4228	***pchD***	-6.1	<1.0E-300	-1.3	1.5E-03	-3.4	<1.0E-300	-1.9	2.4E-04
PA4229	***pchC***	-6.4	3.5E-3086	1.3	3.5E-03	-3.2	1.7E-85	-	-
PA4230	***pchB***	-6.6	<1.0E-300	-5.3	1.1E-04	-3.9	<1.0E-300	-3.0	7.4E-06
PA4231	***pchA***	-6.6	<1.0E-300	-2.0	2.1E-03	-3.8	5.2E-268	-2.8	1.1E-04
PVD pathway									
PA2385	***pvdQ***	-9.4	<1.0E-300	-1.5	9.9E-04	-		-	
PA2386	***pvdA***	-10.2	<1.0E-300	-2.4	1.7E-04	-		-	
PA2389	***pvdR***	-7.6	<1.0E-300	-1.4	2.4E-03	-		-	
PA2390	***pvdT***	-7.6	<1.0E-300	-	-	-		-	
PA2391	***opmQ***	-7.7	<1.0E-300	-2.3	1.0E-03	-		-	
PA2392	***pvdP***	-7.7	<1.0E-300	-3.5	1.2E-05	-		-	
PA2394	***pvdN***	-9.6	<1.0E-300	-2.0	3.3E-04	-		-	
PA2395	***pvdO***	-8.9	<1.0E-300	-2.5	5.5E-05	-		-	
PA2396	***pvdF***	-6.8	<1.0E-300	-3.2	2.7E-05	-		-	
PA2397	***pvdE***	-9.9	<1.0E-300	-2.8	8.4E-04	-		-	
PA2398	***fpvA***	-8.9	<1.0E-300	-2.3	2.0E-04	-		-	
PA2399	***pvdD***	-6.9	<1.0E-300	-0.6	3.8E-02	-		-	
PA2400	***pvdJ***	-6.8	<1.0E-300	-2.2	1.7E-04	-		-	
PA2404	***fpvH***	-5.2	9.5E-287	-	-	-		-	
PA2405	***fpvJ***	-5.2	<1.0E-300	-2.2	1.2E-02	-		-	
PA2406	***fpvK***	-5.5	4.7E-162	-	-	-		-	
PA2407	***fpvC***	-4.9	8.0E-134	-	-	-		-	
PA2408	***fpvD***	-4.9	5.4E-116	-2.1	7.5E-03	-		-	
PA2410	***fpvF***	-4.3	6.9E-162	1.6	2.0E-02	-		-	
PA2413	***pvdH***	-6.7	<1.0E-300	-2.8	7.3E-05	-		-	
PA2424	***pvdL***	-9.3	<1.0E-300	-1.8	1.7E-04	-		-	
PA2426	***pvdS***	-9.9	<1.0E-300	-	-	-		-	

Table 2. Expression values from transcriptomic and proteomic analysis of genes of the PVD and PCH pathways in *P. aeruginosa* PAO1 cells grown in CAA medium with or without 10 µM Fe^{3+} or Co^{2+}. '-' indicates a non-significant difference in expression: -1 < log2 fold change < 1.

Legends of figures

Figure 1: Chemical structure of pyoverdine (PVD) and pyochelin (PCH).

Scheme 1. Organization of PCH pathway genes in the *P. aeruginosa* PAO1 genome. *fptABCX*, *pchEFGHI*, *pchR*, and *pchDCBA* are all genes coding for proteins involved in Fe^{3+} acquisition by PCH. Fur is a transcription regulator. Fur loaded with Fe^{2+} represses the expression of all PCH genes via an interaction with the Fur box. PchR is a transcriptional activator of the AraC family. PchR in complex with PCH-Fe^{3+} activates the transcription of all PCH genes, except *pchR*, by interacting with the PchR box (no PchR box upstream of *pchR*).[21–23]

Figure 2. PVD (A) and PCH (B) production by *P. aeruginosa* PAO1 in the absence and presence of different biological metals. Bacteria were grown 24 h in CAA medium with or without 1, 15, or 150 µM of biological metals (no metal (control): black; $FeCl_3$: red; $CoCl_2$: pink; $NiCl_2$: blue; $CuCl_2$: yellow; $MnCl_2$: purple and $ZnCl_2$: green). The concentration of PVD and PCH (µM/$OD_{600\,nm}$) was monitored after 24 h in culture and calculated as described in Materials and Methods.

Figure 3. **A. Analysis of fold-change in transcription for genes of the PVD and PCH pathways.** *pvdS* and *pvdJ* genes encode a sigma factor and an enzyme involved in PVD pathway. The oder five gens belong to the PVD pathway: *pchR*, encodes the transcriptional regulator, *pchA* and *pchE* are NRPS involved in PCH biosynthesis and *fptA* and *fptX* the outer and inner membrane transporters of PCH-Fe, respectively. RT-qPCR was performed on *P. aeruginosa* PAO1 grown in CAA medium with or without 5 µM $FeCl_3$, $CoCl_2$, $NiCl_2$ or $ZnCl_2$. The data were normalized relative to the reference gene *uvrD* and are representative of three independent experiments. Results are given as a ratio between the values obtained in the presence of metals over those obtained in the absence. All values fold-change values are given in Table 3SM in Supplemental Materials.

B. PchA-mCherry, PchE-mCHERRY and FptX-mCHERRY expression in *P. aeruginosa* cells grown in CAA medium with or without 5 µM $FeCl_3$, $CoCl_2$, $NiCl_2$ or $ZnCl_2$. *pchA-mcherry*, *pchE-mcherry* and *fptX-mcherry* strains were grown in CAA medium. The metals were added at the beginning of culture and bacterial growth monitored at $OD_{600\ nm}$ and the expression of the fluorescent fusion proteins measured by following the fluorescence at 610 nm (excitation at 570 nm). All kinetics are an average of 5 kinetics.

C. mCHERRY-PchR expression in *P. aeruginosa* cells grown in CAA medium with or without $FeCl_3$, $CoCl_2$ or $NiCl_2$. Since the emission of fluorescence in *mcherry-pchR* strain and the variation of fluorescence observed in the presence of Fe^{3+} are low, different metal concentrations were tested. The metals were added at the beginning of culture and bacterial growth monitored at $OD_{600\ nm}$ and the expression of the fluorescent fusion proteins measured by following the fluorescence at 610 nm (excitation at 570 nm). All kinetics are an average of 5 kinetics

Figure 4. A. Transport of PCH-Fe and PCH-Co in *P. aeruginosa* cells. Δ*pvdF*Δ*pchA* (grey bars) and *ΔpvdFΔpchAΔfptA* (white bars) strains at an $OD_{600\ nm}$ of 1 in CAA medium were incubated with or without 4 µM of preformed PCH-metal complexes. For both panels, bacteria were pelleted after a 30-min incubation, washed, and the amount of metal monitored by ICP-AES. **B. Kinetics of intracellular ^{55}Fe accumulation in *P. aeruginosa* cells in the presence of PCH-metal complexes.** Δ*pvdF*Δ*pchA* cells at an $OD_{600\ nm}$ of 1 were incubated with 0.2 µM PCH-^{55}Fe and without (black dots) or with 1 eq. (0.2 µM) or 10 eq. (2 µM) PCH-metal complexes (PCH-Co in green, PCH-Ni in blue, or PCH-Zn in orange). Aliquots were removed at various times and the radioactivity in the cells monitored.

Figure 5. Total content of biological metals in *P. aeruginosa* PAO1 cells grown in CAA medium with or without 5 µM $CoCl_2$. *P. aeruginosa* PAO1 cells were grown in CAA medium without (grey bars) or with 5 µM $CoCl_2$ (black bars). The data are expressed as moles per volume as described previously.[13] The absence of columns for some metals corresponds to the detection limits for low-abundance

elements under these experimental conditions. For all experiments, bacteria were grown in CAA, harvested at the end of the exponential phase, and prepared for ICP-AES measurements as described in Materials and Methods.

Figure 6. Electrophoretic mobility shifts of specific 41bp DNA fragments (g -65 to -31 *pchD* gene promoter containing a Fur box) incubated with Fur protein in the presence of 10 µM $CoCl_2$ or $Mn(OAc)_2$. See the experimental part for details. It is not possible to run EMSA in presence of Fe^{2+} because of its oxidation, consequently, it is well accepted in the literature to use manganese ions to mimic Fe^{2+} for the DNA binding assay.[52]

Figure 7. Expression of mCherry from the pAYC5 plasmid in the absence or presence of $FeCl_3$, $CoCl_2$, $NiCl_2$, or $ZnCl_2$ under Fur regulation. Δ*pchR* cells were transformed with pAYC5 plasmid carrying the *pchD* promoter sequence with the Fur and PchR boxes. These cells were grown in the presence of increasing concentrations of $FeCl_3$, $CoCl_2$, $NiCl_2$ or $ZnCl_2$ (see legend on figure). Bacterial growth was followed at $OD_{600\ nm}$ and mCherry expression by monitoring the emission of fluorescence at 610 nm (excitation at 570 nm).

Figure 8. Expression of mCherry from pAYC5-FURmut plasmid in the absence or presence of $FeCl_3$, $CoCl_2$, $NiCl_2$ or $ZnCl_2$ under PchR regulation. PAO1 (all kinetics with the symbol ● in panels A, B, C and D) and Δ*pchR* (kinetics in grey with the symbol ▲ in panels A, B, C and D) cells were transformed with pAYC5-FURmut plasmid carrying the *pchD* promoter sequence with the PchR box and a Fur mutated box. These cells were grown in CAA medium in the presence of increasing concentrations of $FeCl_3$, $CoCl_2$, $NiCl_2$ or $ZnCl_2$. Bacterial growth was followed at $OD_{600\ nm}$ and mCherry expression by monitoring the emission of fluorescence at 610 nm (excitation at 570 nm). All kinetics are an average of 5 kinetics. No significant variation of mCherry expression was observed in Δ*pchR* mutant in the presence of metals as shown in Supplemental Materials, Figure 4SM.

Scheme 2. The PCH pathway and its interaction with Fe^{3+} and Co^{2+}. PCH can chelate both Fe^{3+} and Co^{2+}. FptA at the bacterial cell surface can interact with both PCH-metal complexes, but with the highest affinity for PCH-Fe, and both complexes are transported efficiently into *P. aeruginosa* cells. The biological function of Fur is not affected by the presence of contaminant Co^{2+} in the bacterial growth medium. PchR can bind PCH-Fe and PCH-Co as well as PCH-Ni, and PCH-Zn, but only PchR-PCH-Fe activates the transcription of PCH genes. The presence of contaminant Co^{2+} in the bacteria growth media leads to the formation of PchR-PCH-Co complexes. This will decrease the intracellular concentration of PchR-PCH-Fe, leading to a decrease in the expression of PCH genes and PCH production.

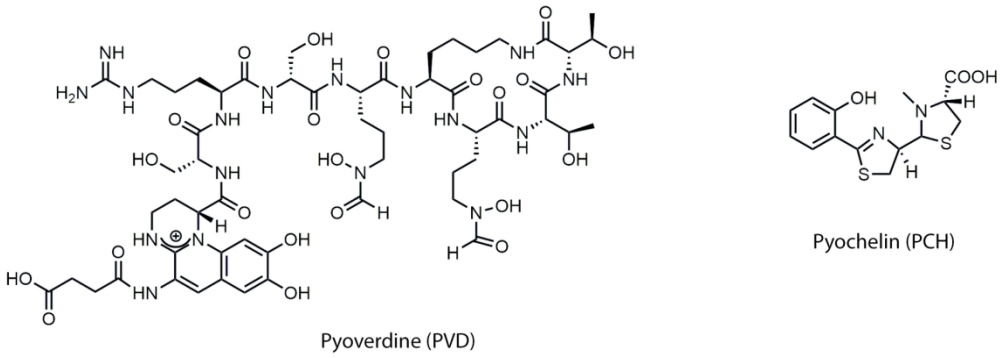

Figure 1: Chemical structure of pyoverdine (PVD) and pyochelin (PCH).

159x57mm (300 x 300 DPI)

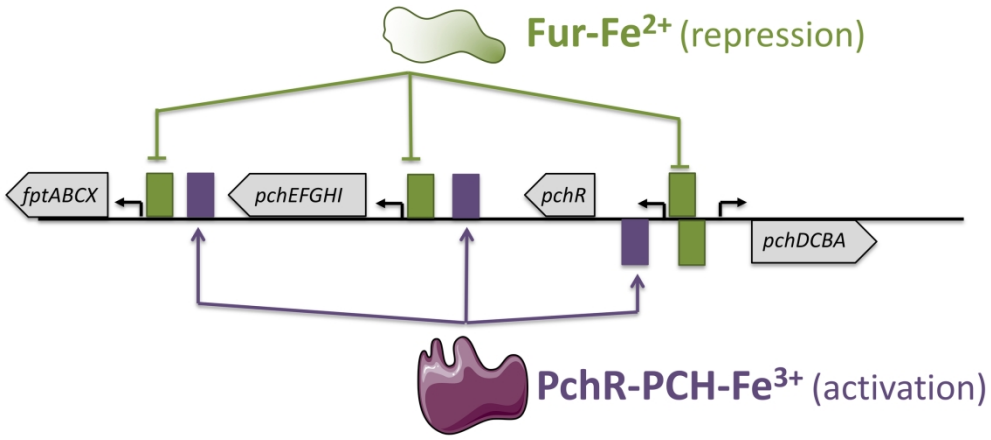

Scheme 1. Organization of PCH pathway genes in the *P. aeruginosa* PAO1 genome. *fptABCX*, *pchEFGHI*, *pchR*, and *pchDCBA* are all genes coding for proteins involved in Fe^{3+} acquisition by PCH. Fur is a transcription regulator. Fur loaded with Fe^{2+} represses the expression of all PCH genes via an interaction with the Fur box. PchR is a transcriptional activator of the AraC family. PchR loaded with PCH-Fe^{3+} activates the transcription of all PCH genes, except *pchR*, by interacting with the PchR box (no PchR box upstream of pchR).[21–23]

220x100mm (300 x 300 DPI)

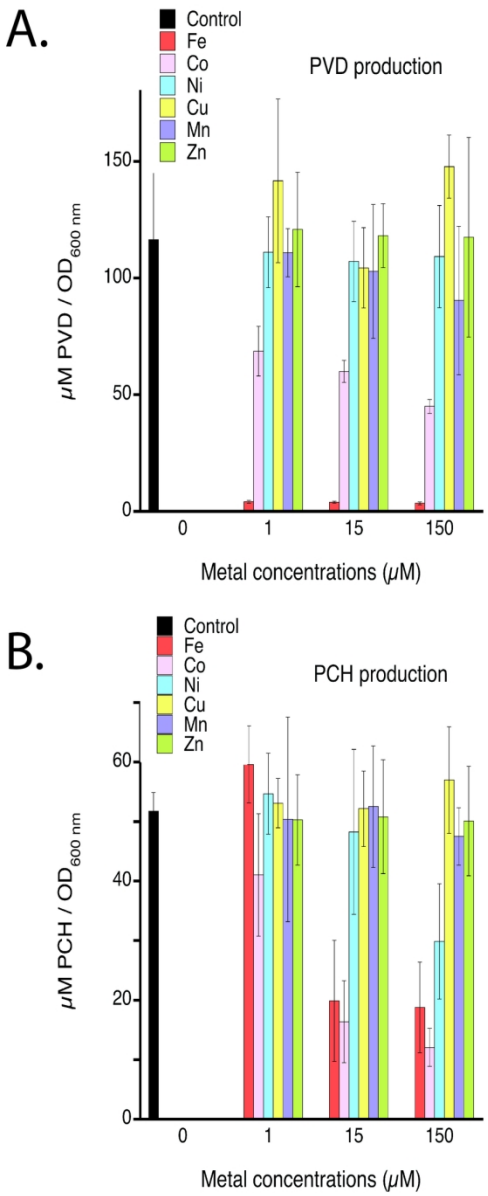

Figure 2. PVD (A) and PCH (B) production by *P. aeruginosa* PAO1 in the absence and presence of different biological metals. Bacteria were grown 24 h in CAA medium with or without 1, 15, or 150 µM of biological metals (no metal (control): black; $FeCl_3$: red; $CoCl_2$: pink; $NiCl_2$: blue; $CuCl_2$: yellow; $MnCl_2$: purple and $ZnCl_2$: green). The concentration of PVD and PCH ($\mu M/OD_{600\ nm}$) was monitored after 24 h in culture and calculated as described in Materials and Methods.

80x194mm (300 x 300 DPI)

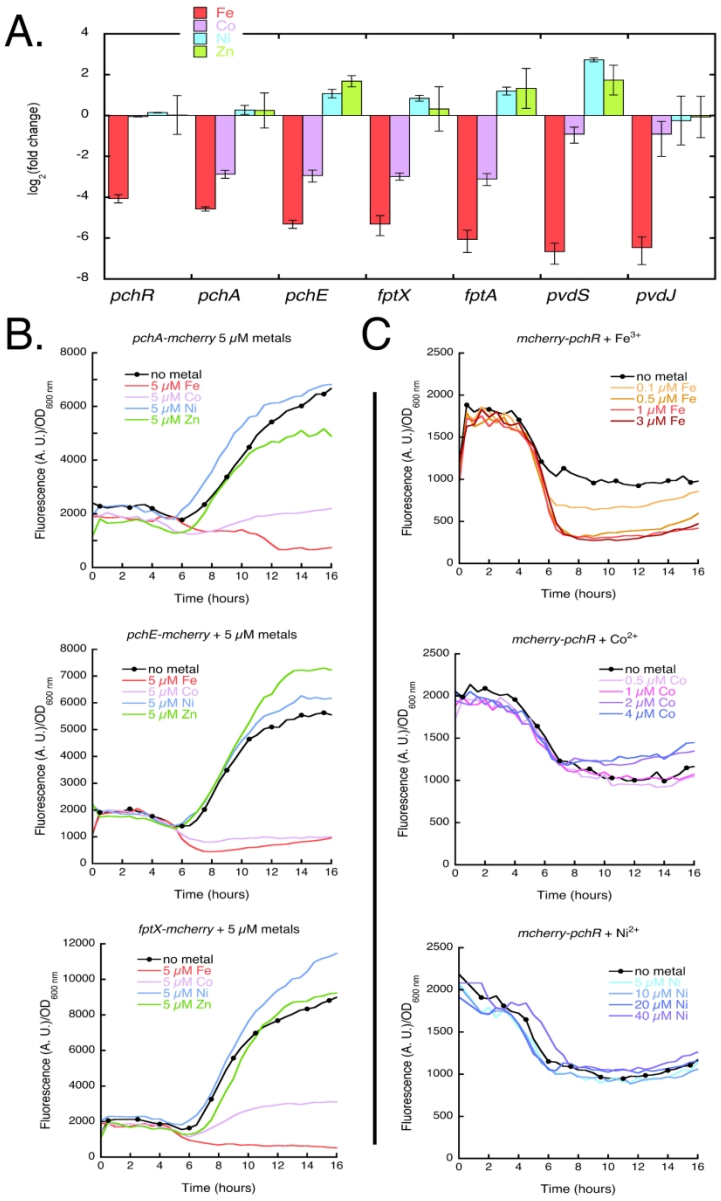

Figure 3. A. Analysis of fold-change in transcription for genes of the PVD and PCH pathways. *pvdS* and *pvdJ* genes encode a sigma factor and an enzyme involved in PVD pathway. The oder five gens belong to the PVD pathway: *pchR*, encodes the transcriptional regulator, *pchA* and *pchE* are NRPS involved in PCH biosynthesis and *fptA* and *fptX* the outer and inner membrane transporters of PCH-Fe, respectively. RT-qPCR was performed on *P. aeruginosa* PAO1 grown in CAA medium with or without 5 µM $FeCl_3$, $CoCl_2$, $NiCl_2$ or $ZnCl_2$. The data were normalized relative to the reference gene *uvrD* and are representative of three independent experiments. Results are given as a ratio between the values obtained in the presence of metals over those obtained in the absence. All values fold-change values are given in Table 3SM in Supplemental Materials. "B. PchA-mCherry, PchE-mCHERRY and FptX-mCHERRY expression in *P. aeruginosa* cells grown in CAA medium with or without 5 µM $FeCl_3$, $CoCl_2$, $NiCl_2$ or $ZnCl_2$. *pchA-mcherry*, *pchE-mcherry* and *fptX-mcherry* strains were grown in CAA medium. The metals were added at the beginning of culture and bacterial growth monitored at $OD_{600\ nm}$ and the expression of the fluorescent fusion proteins measured by following the fluorescence at 610 nm (excitation at 570 nm). All kinetics are an average of 5 kinetics."C. mCHERRY-PchR

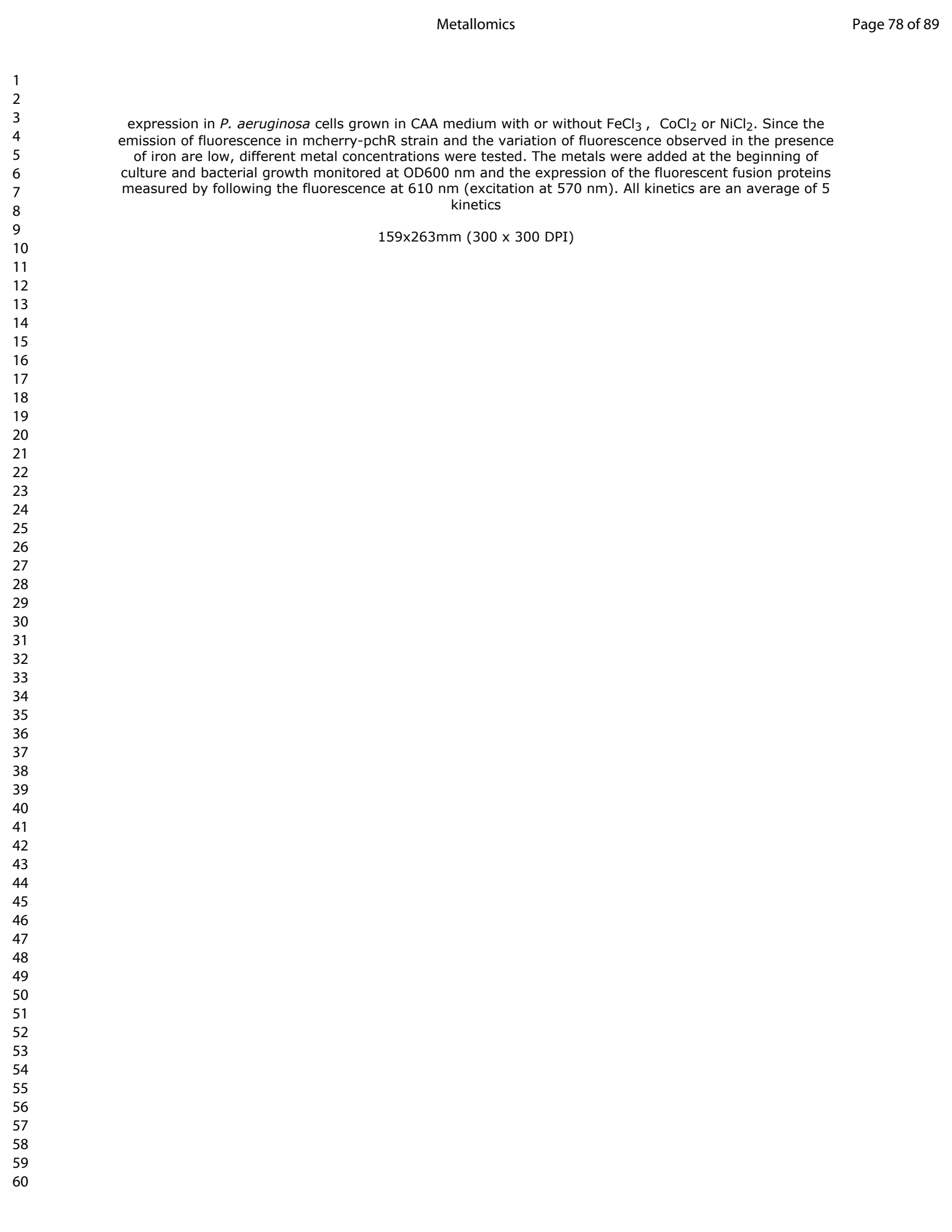

expression in *P. aeruginosa* cells grown in CAA medium with or without $FeCl_3$, $CoCl_2$ or $NiCl_2$. Since the emission of fluorescence in mcherry-pchR strain and the variation of fluorescence observed in the presence of iron are low, different metal concentrations were tested. The metals were added at the beginning of culture and bacterial growth monitored at OD600 nm and the expression of the fluorescent fusion proteins measured by following the fluorescence at 610 nm (excitation at 570 nm). All kinetics are an average of 5 kinetics

159x263mm (300 x 300 DPI)

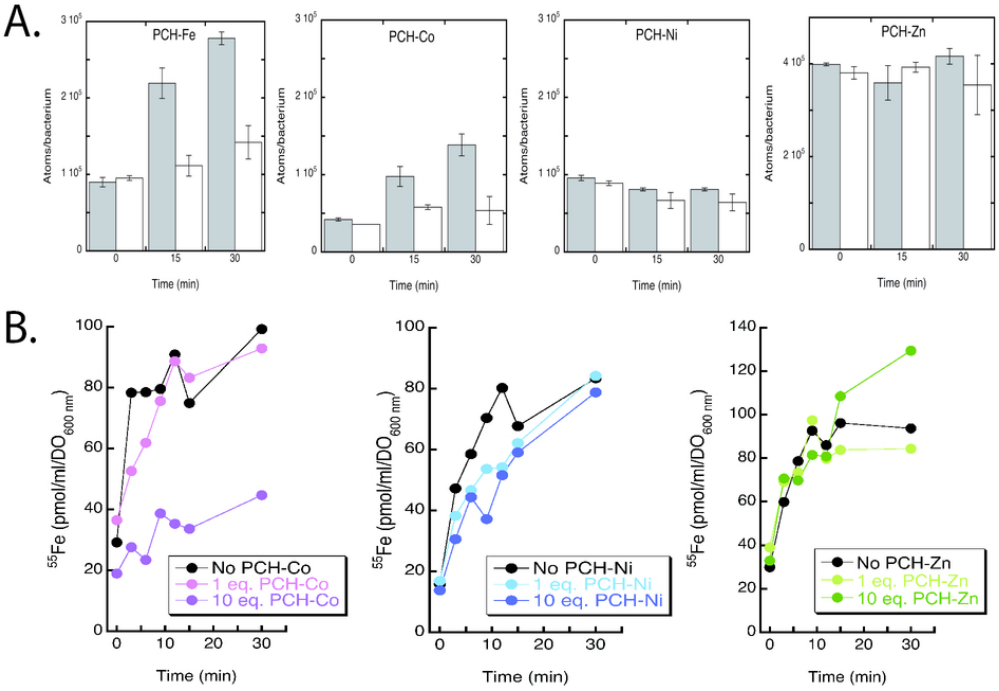

Figure 4. A. Transport of PCH-Fe and PCH-Co in *P. aeruginosa* cells. Δ*pvdF*Δ*pchA* (grey bars) and Δ*pvdF*Δ*pchA*Δ*fptA* (white bars) strains at an $OD_{600\ nm}$ of 1 in CAA medium were incubated with or without 4 µM of preformed PCH-metal complexes. For both panels, bacteria were pelleted after a 30-min incubation, washed, and the amount of metal monitored by ICP-AES. B. Kinetics of intracellular ^{55}Fe accumulation in *P. aeruginosa* cells in the presence of PCH-metal complexes. Δ*pvdF*Δ*pchA* cells at an $OD_{600\ nm}$ of 1 were incubated with 0.2 µM PCH-^{55}Fe and without (black dots) or with 1 eq. (0.2 µM) or 10 eq. (2 µM) PCH-metal complexes (PCH-Co in green, PCH-Ni in blue, or PCH-Zn in orange). Aliquots were removed at various times and the radioactivity in the cells monitored.

80x55mm (300 x 300 DPI)

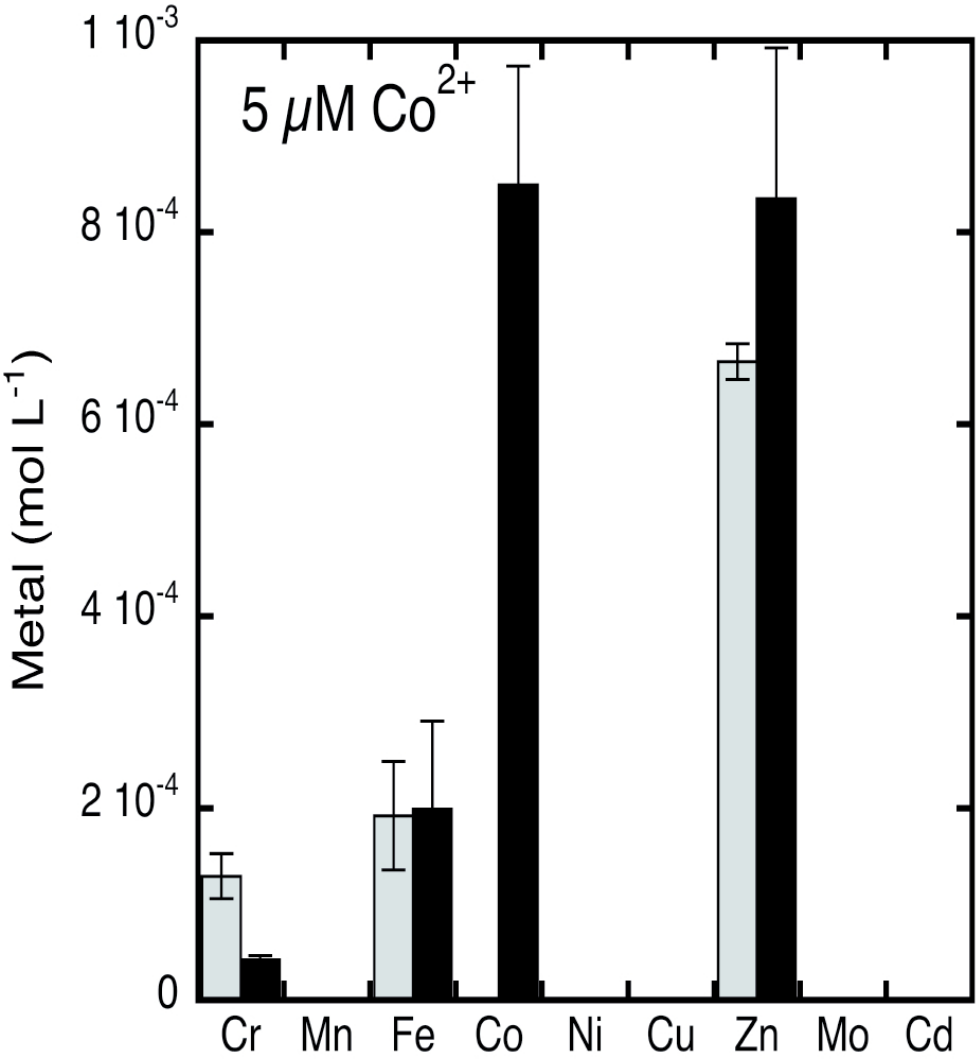

Figure 5. Total content of biological metals in *P. aeruginosa* PAO1 cells grown in CAA medium with or without 5 μM $CoCl_2$. *P. aeruginosa* PAO1 cells were grown in CAA medium without (grey bars) or with 5 μM $CoCl_2$ (black bars). The data are expressed as moles per volume (Log representation) as described previously.[13] The absence of columns for some metals corresponds to the detection limits for low-abundance elements under these experimental conditions. For all experiments, bacteria were grown in CAA, harvested at the end of the exponential phase, and prepared for ICP-AES measurements as described in Materials and Methods.

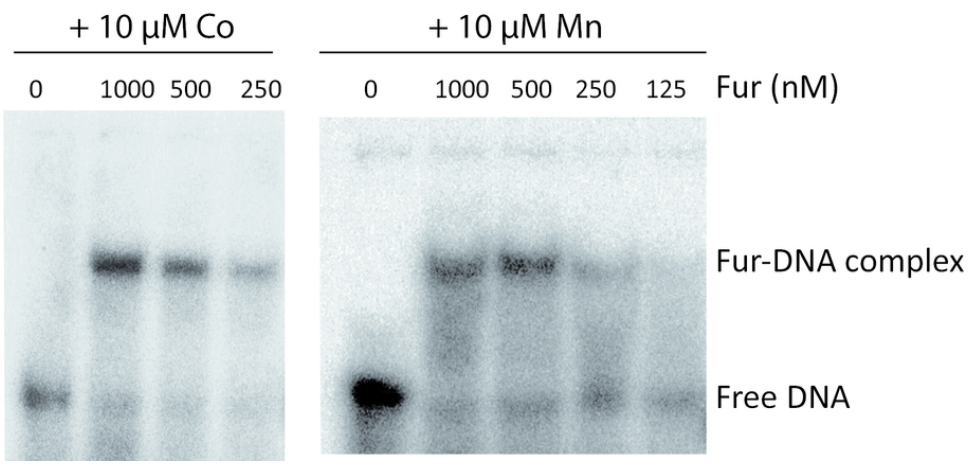

Figure 6. Electrophoretic mobility shifts of specific 41bp DNA fragments (g -65 to -31 pchD gene promoter containing a Fur box) incubated with Fur protein in the presence of 10 µM Co^{2+} or Mn^{2+}. See the experimental part for details. It is not possible to run EMSA in presence of ferrous iron because of its oxidation, consequently, it is well accepted in the literature to use manganese ions to mimic ferrous iron for the DNA binding assay.[52]

80x36mm (300 x 300 DPI)

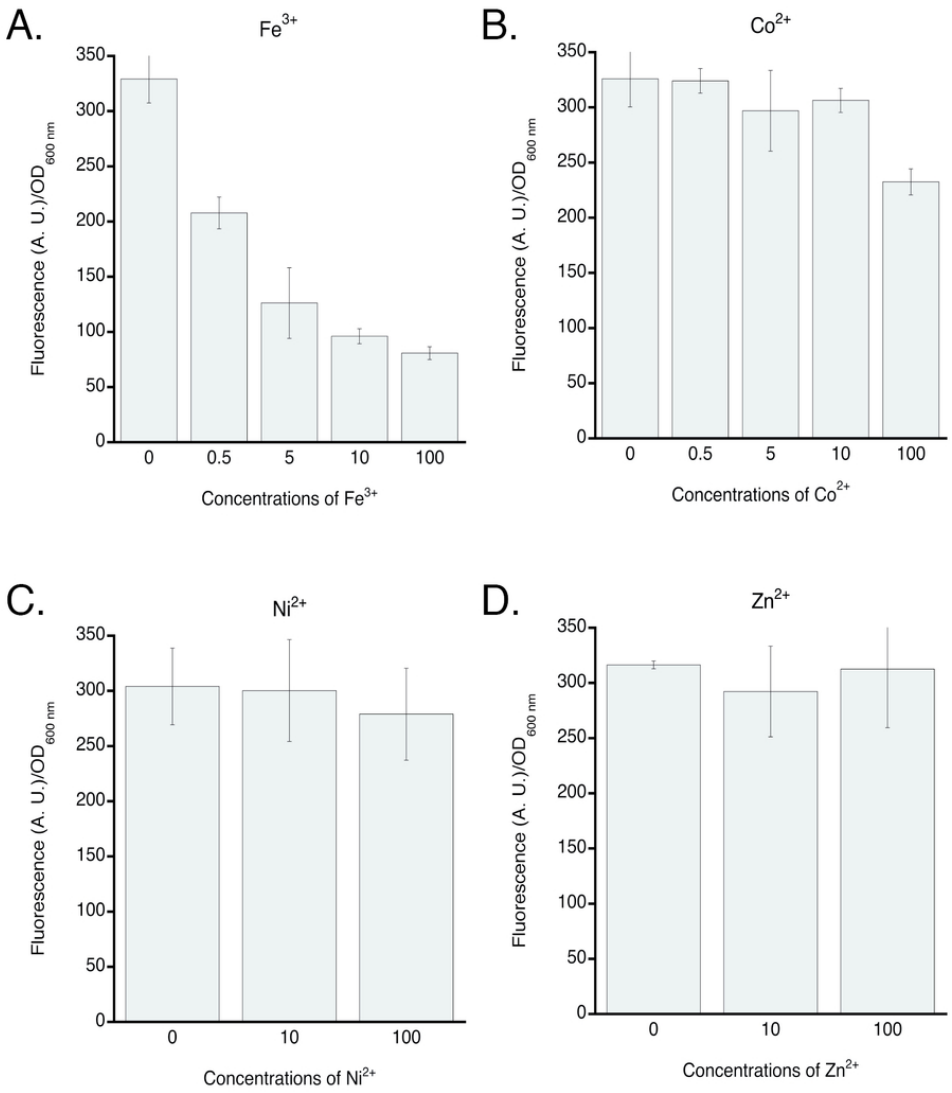

Figure 7. Expression of mCherry from pAYC5 plasmid in the absence or presence of $FeCl_3$, $CoCl_2$, $NiCl_2$, or $ZnCl_2$ under Fur regulation. Δ*pchR* cells were transformed with pAYC5 plasmid carrying the *pchD* promoter sequence with the Fur and PchR boxes. These cells were grown in the presence of increasing concentrations of $FeCl_3$, $CoCl_2$, $NiCl_2$ or $ZnCl_2$ (see legend on figure). Bacterial growth was followed at $OD_{600\ nm}$ and mCherry expression by monitoring the emission of fluorescence at 610 nm (excitation at 570 nm).

79x87mm (300 x 300 DPI)

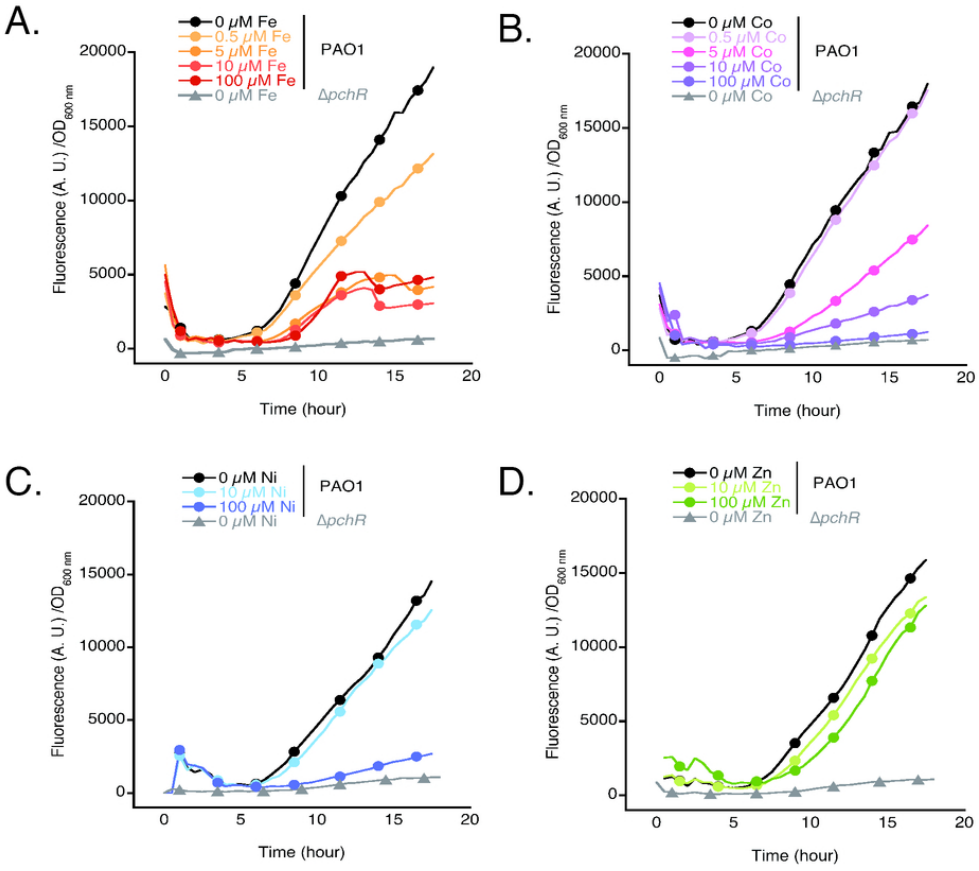

Figure 8. Expression of mCherry from pAYC5-FURmut plasmid in the absence or presence of $FeCl_3$, $CoCl_2$, $NiCl_2$ or $ZnCl_2$ under PchR regulation. PAO1 (all kinetics with the symbol • in panels A, B, C and D) and Δ*pchR* (kinetics in grey with the symbol ▵ in panels A, B, C and D) cells were transformed with pAYC5-FURmut plasmid carrying the *pchD* promoter sequence with the PchR box and a Fur mutated box. These cells were grown in CAA medium in the presence of increasing concentrations of $FeCl_3$, $CoCl_2$, $NiCl_2$ or $ZnCl_2$. Bacterial growth was followed at $OD_{600\ nm}$ and mCherry expression by monitoring the emission of fluorescence at 610 nm (excitation at 570 nm). All kinetics are an average of 5 kinetics. No significant variation of mCherry expression was observed in Δ*pchR* mutant in the presence of metals as shown in Supplemental Materials, Figure 4SM.

79x69mm (300 x 300 DPI)

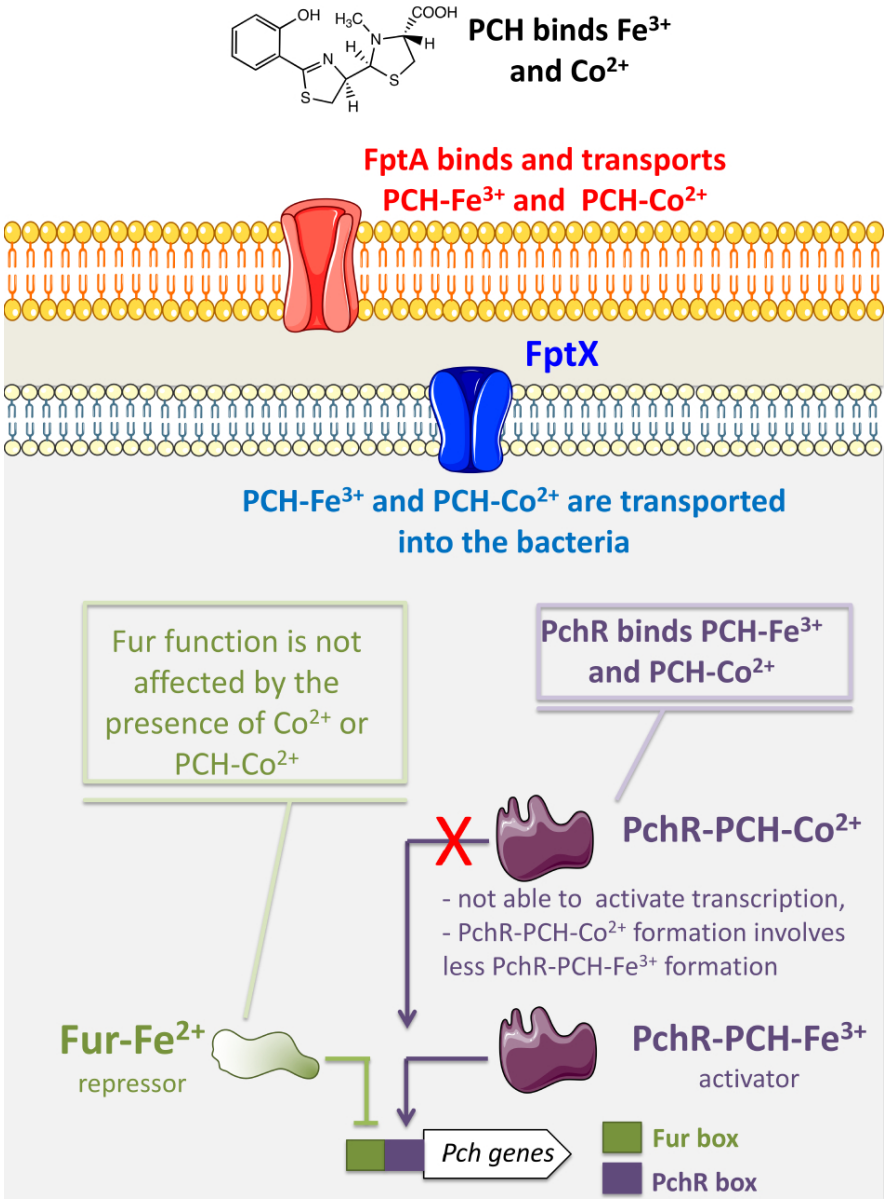

Scheme 2. The PCH pathway and its interaction with Fe3+ and Co^{2+}. PCH can chelate both Fe^{3+} and Co^{2+}. FptA at the bacterial cell surface can interact with both PCH-metal complexes, but with the highest affinity for PCH-Fe, and both complexes are transported efficiently into *P. aeruginosa* cells. The biological function of Fur is not affected by the presence of contaminant Co^{2+} in the bacterial growth medium. PchR can bind PCH-Fe and PCH-Co as well as PCH-Ni, and PCH-Zn, but only PchR-PCH-Fe activates the transcription of PCH genes. The presence of contaminant Co^{2+} in the bacteria growth media leads to the formation of PchR-PCH-Co complexes. This will decrease the intracellular concentration of PchR-PCH-Fe, leading to a decrease in the expression of PCH genes and PCH production.

80x109mm (300 x 300 DPI)

Supplemental Support

Nonspecific interference of cobalt with siderophore-dependent iron uptake pathways

Ana Carballido Lopez[a,b], Olivier Cunrath[a,b], Anne Foster[a,b], Julien Pérard[c], Gwenaëlle Graulier[a,b], Rachel Legendre[d,e], Hugo Varet[d,e], Odile Sismeiro[d], Quentin Perraud[a,b], Bénédicte Pesset[a,b], Pamela Saint Auguste[6], Dirk Bumann[6], Gaëtan L. A. Mislin[a,b], Jean Yves Coppee[d], Isabelle Michaud-Soret[c], Pierre Fechter*[a,b] and Isabelle J.Schalk*[a,b]

Promotor regions	Sequences	Gene localisation
PchR box	5'GACAAAGCGCCCTGCACTCCGCCCCTGCAG CGAATGAAAAAGCCCCGCAATCGAAAGGCGC GGGCTTGCGCGGT3'	4742278 -
Fur box	5'CCCTGCCGCCCGCCAATGATAATAAATCTCA TTTCCCAACAATGGCAATCGACCGCATCCACG GAGATCGCATG 3'	4742426 [+]
Fur box	5'GCCGCCCGCCAATGATAATAAATCTCATTTC CCAACAATGGCAATCGACCGCATCCACGGAG ATCGCATG 3'	4742356 - 4742426 [+]

Table 1SM. ***pchD* promoter sequences introduced into pAYC5 vector for the construction of expression plasmids carrying mCherry.** See 'Material and methods'. Red sequence correspond to the PchR box, and blue sequences to the Fur box. The genome location in PAO1 is according to www.pseudomonasaeruginosa.com.

Oligonucleotides	Sequences (5' to 3')	Used to construct the following plasmids or in RT-qPCR
pchD prom F	CAAAGAATTCGACAAAGCGCCCTGCACTCCG	pAYC5
pchD prom R	CATGTTATCCTCCTCGCCCTTGCTCACCATGCGATCTCCGTGGATGCG	
	GTGAGCAAGGGCG*AG*GAGGATAACATG	
mcherry F	CTCCAAGCTTTTACTTGTACAGCTCGTCCATGCCGC	
mcherry R		
MutFur F	TAATAAATCT*gtaa*TCCCAACAATGGCAATCGACCGCTGCACCGCATCC	pAYC5-FURmut
	ACGGAG	
MutFur R	TCATTGGCGGGCGGCAGG	
uvrD F	CTACGGTAGCGAGACCTACAACAA	RT-qPCR
uvrD R	GCGGCTGACGGTATTGGA	RT-qPCR
pchA F	CGCGAAACCTGCCTTAAGC	RT-qPCR
pchA R	GTCCAGGCCGCCTATGG	RT-qPCR
pchE F	GGCAATGGCAAGGTCGAT	RT-qPCR
pchE R	CACCGGGCGTTTGAGAAC	RT-qPCR
pvdS F	CAGGCGCTCGAACAGAAATA	RT-qPCR
pvdS R	CGTAGTTGATGTGCGAGGTT	RT-qPCR
pvdJ F	CGTGGCCGCGATATGG	RT-qPCR
pvdJ R	CTCTTCAGGCTGACTTCGATACC	RT-qPCR
fptA F	CGTGGCCGCGATATGG	RT-qPCR
fptA R	CTCTTCAGGCTGACTTCGATACC	RT-qPCR
fptX F	CCCTGGGTGGTCAAGTTCCT	RT-qPCR
fptX R	CGGCGCGACCAGTGA	RT-qPCR
pchR R	GCGCCTGGGCTACAAGATC	RT-qPCR
pchR F	CCGTAGCGGTTGTTCCAGTT	RT-qPCR

Table 2SM: Oligonucleotides used in this study. The mutated residues in pAYC5-FURmut vector are in non-capital letters.

	$FeCl_3$	$CoCl_2$	$NiCl_2$	$ZnCl_2$
pchR	0.06645985	0.954978494015707	1.49665264	1.98795531
	0.06252901	0.957584025403966	1.25575259	0.08943202
	0.05072588	0.965450446181038	0.55587927	0.97924892
Mean	0.05990491	0.95933766	1.1027615	1.01887875
pchA	0.04346023	0.15771836	2.20764985	2.18134132
	0.04409012	0.12956486	0.68718696	0.26671069
	0.03869765	0.12376815	0.72774352	1.11181292
Mean	0.04208267	0.13701712	1.20752678	1.18662164
pchE	0.02923664	0.11095663	3.194277	3.97225907
	0.02285894	0.16083733	1.30681679	2.8159316
	0.02354194	0.12079607	1.79714278	2.8159316
Mean	0.02521251	0.13086334	2.09941219	3.20137409
fptX	0.03483301	0.12469778	1.90421623	3.109841
	0.02094053	0.14288368	0.83928485	0.31812839
	0.01999315	0.11268389	1.00482262	1.95459969
Mean	0.02525556	0.12675512	1.24944123	1.7941897
fptA	0.02091847	0.1345655	4.21045052	5.19471528
	0.01371907	0.12324825	1.04553504	0.49657243
	0.01028649	0.09012936	1.62044297	1.82430115
Mean	0.01497468	0.11598104	2.29214284	2.50519629
pvdS	0.01311133	0.68277492	8.2598626	5.49103089
	0.00995599	0.51011365	1.98679923	1.10294092
	0.00636272	0.40394858	9.59973623	3.37346338
Mean	0.00981001	0.53227905	6.61546602	3.32247839
pvdJ	0.01700111	0.76043686	1.53870177	2.04157712
	0.0082309	0.62422786	0.39201924	0.1898839
	0.008663	0.21540189	0.59857482	0.62539424
Mean	0.01129834	0.53335554	0.84309861	0.95228508

Table 3SM: Experimental data of RT-qPCR experiment presented in Figure 3A.

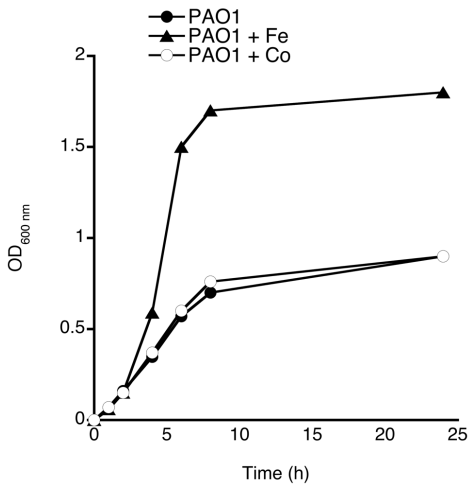

Figure 1SM: Growth curve of PAO1 grown in CAA medium in the absence and presence of 10 µM Fe^{3+} or Co^{2+}. Growth conditions used for proteomic and transcriptomic analyses.

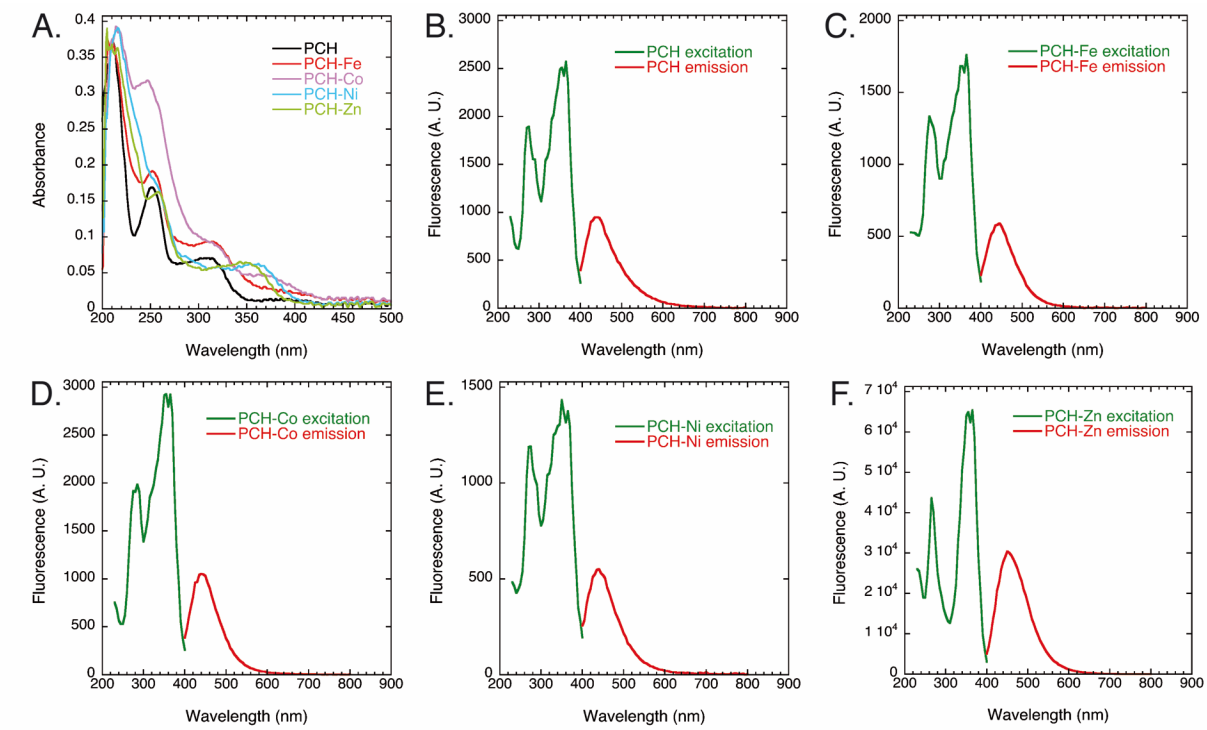

Figure 2SM: A. UV spectra of apo PCH and PCH-metal complexes recorded in 50 mM TrisHCl pH 8.0. **B-F.** Superposition of the normalized emission (red) and excitation (green) spectra recorded in 50 mM TrisHCl pH 8.0 for apo PCH and the different PCH-metal complexes. Emission spectra : λ_{exc} = 350 nm; excitation spectra : λ_{em} = 422 nm.

The complexes have been prepared as described in Materials and Methods by mixing 1 equivalent of metal with 2 equivalents of PCH. UV and fluorescence spectra of apo PCH were carried out at 100 µM for apo PCH and at 50 µM for the PCH-metal complexes. The fluorescence emission scale is not the same in panels B-F: PCH-Zn is much more fluorescent than apo PCH and the other PCH-metal complexes; for PCH-Fe and PCH-Ni the fluorescence is slightly quenched. Apo PCH and PCH-Ni have both a maximum of fluorescence at 438 nm, PCH-Fe at 443 nm, PCH-Co at 440 and PCH-Zn at 452 nm.

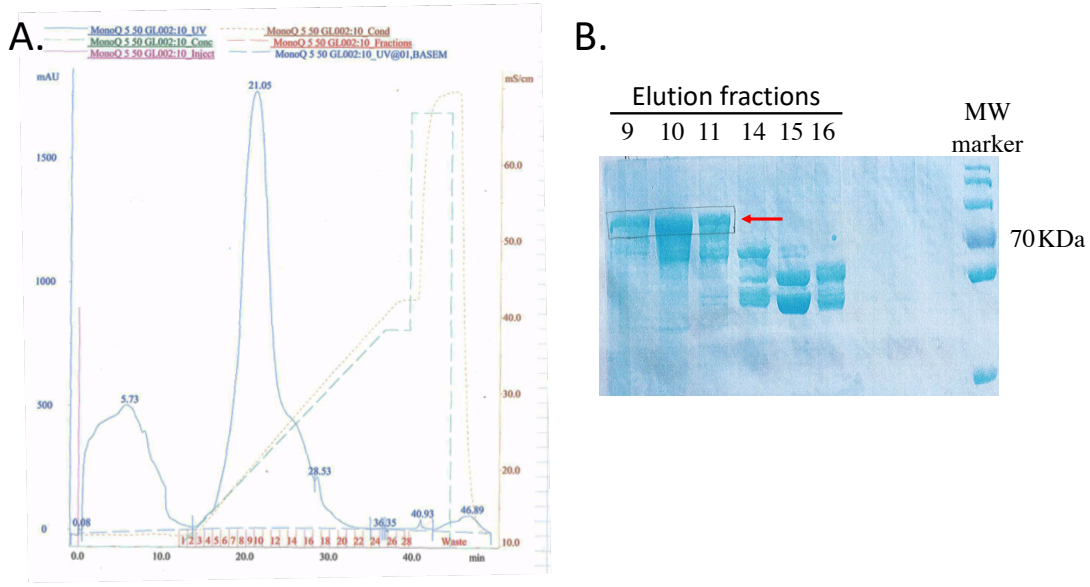

Figure 3SM: MBP-PchR purification. For detailed protocol see in Materials and Methods. **A.** Ionic exchange chromatogram of MBP-PchR (Mono Q™ 5/50 GL). MBP-PchR was eluted with a $NaCl_2$ gradient. **B.** SDS-PAGE analysis of the elution peak at 21 min. MBP-PchR has a molecular weight of 75 kDa and was detected in fractions 9-11.

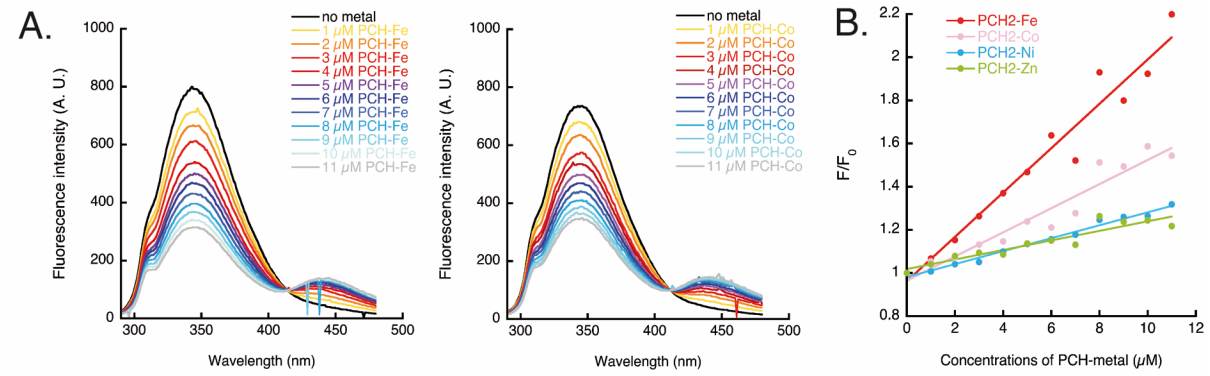

Figure 4SM: A. Fluorescence emission spectra of MBP-PchR in the presence of different PCH-Fe or PCH-Co concentrations. MBP-PchR has a maximal fluorescence emission at 343 nm (black line, excitation at 280 nm). Its fluorescence was quenched with addition of increasing concentrations of PCH-Fe or PCH-Co. PCH-Fe and PCH-Co have a maximal fluorescence emission at 440 nm.
B. Stern-Volmer plot for siderophore binding affinity determination of MBP-PchR. Relative fluorescence intensity (F_0/F) of MBP-PchR at 343 nm in the presence of PCH-Fe, PCH-Co, PCH-Ni and PCH-Zn were plotted against PCH-metal concentrations. Data were fit with a linear regression.

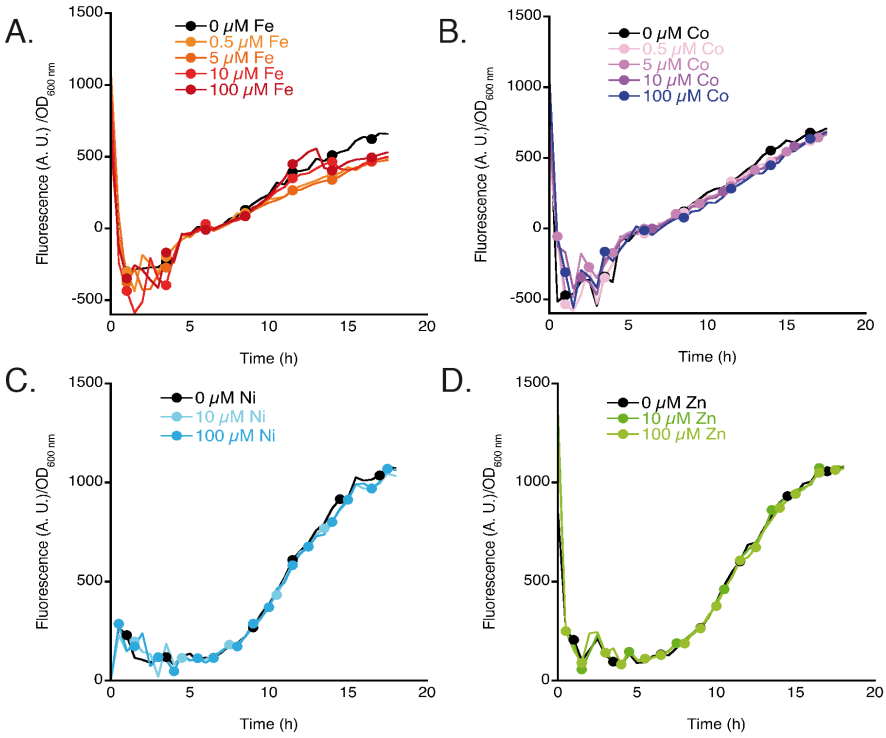

Figure 5SM: Expression of mCherry from pAYC5-FURmut plasmid in the absence or presence of Fe^{3+}, Co^{2+}, Ni^{2+} or Zn^{2+} under Fur regulation in the Δ*pchR* mutant. Δ*pchR* cells were transformed with pAYC5-FURmut plasmid carrying the *pchD* promoter sequence with the PchR box and a Fur mutated box. These cells were grown in CAA medium as PAO1 cells in Figure 7 in the presence of increasing concentrations of Fe^{3+}, Co^{2+}, Ni^{2+} or Zn^{2+}. Bacterial growth was followed at $OD_{600\ nm}$ and mCherry expression by monitoring the emission of fluorescence at 610 nm (excitation at 570 nm). All kinetics are an average of 5 kinetics.